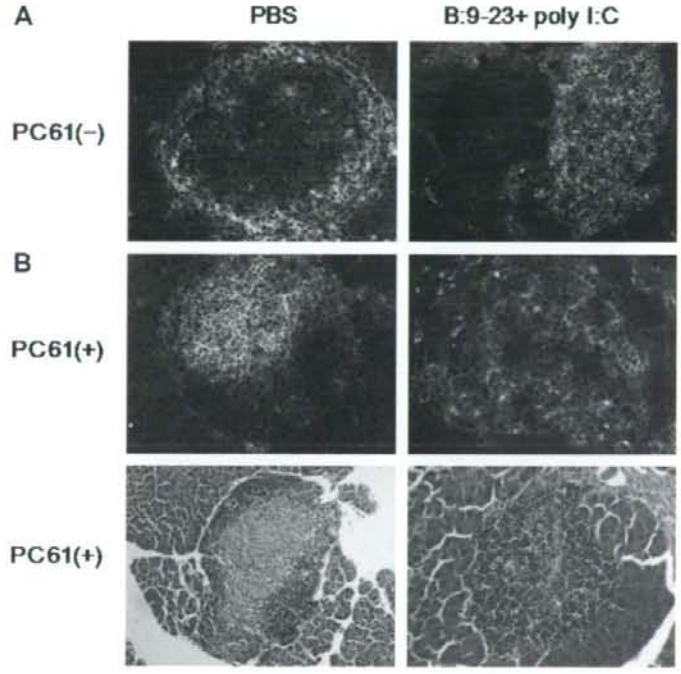

Fig. 2. (A) Immunofluorescence of the sections of pancreata from NOD mice at 6 weeks of age treated with PBS or B:9-23 + poly I:C without PC61 pre-treatment stained with anti-Foxp3 Ab and anti-CD4 mAbs, followed by goat anti-rabbit IgG Alexa555 (red) and goat anti-rat IgG Alexa488 (green). Original magnification: 100×. (B) Immunofluorescence of the sections stained and H&E stained paraffin sections of the pancreas from NOD mice at 6 weeks of age treated with PC61(+) PBS or PC61(+) B:9-23+poly I:C 2 weeks before. Original magnification: 200×.

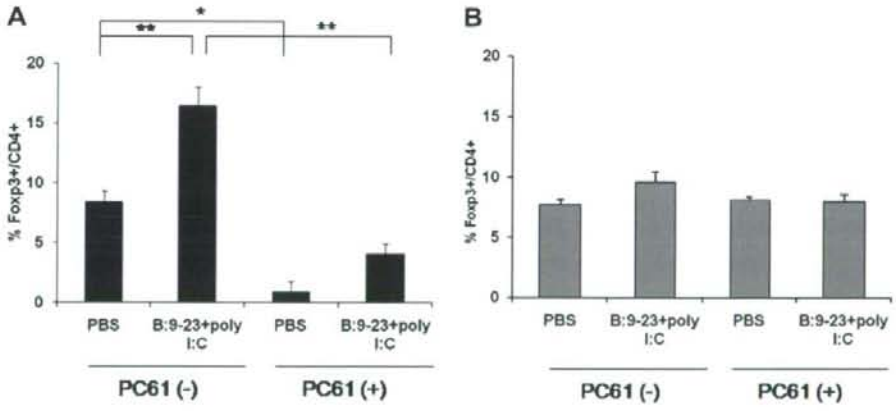

Fig. 3. The numbers of $Foxp3^+$ T cells and $CD4^+$ T cells were counted in several non-consecutive microscopic fields within the T cell area of the pancreas or pancreatic lymph nodes (PLN). The frequency of $Foxp3^+$ T cells in whole $CD4^+$ cells in the T cell area of the pancreas (A) or PLN (B) were compared within each group of treated mice, respectively. The results are presented as means ± SE. $^*P < 0.005$, $^{**}P < 0.0005$.

PBS) and in those treated with B:9-23 peptide and poly I:C ($P < 0.0005$ vs. PC61(−) B:9-23 + poly I:C) (Figs. 2B and 3A). In the PLNs, in contrast, the frequency of $CD4^+Foxp3^+$ T cells was not influenced by treatment with PC61 ($P = 0.954$ vs. PC61(−) PBS) ($P = 0.613$ vs. PC61(−) B:9-23 + poly I:C) (Fig. 3B).

Massive infiltration of lymphoid cells was observed in the islets from mice treated with PC61, B:9-23 peptide

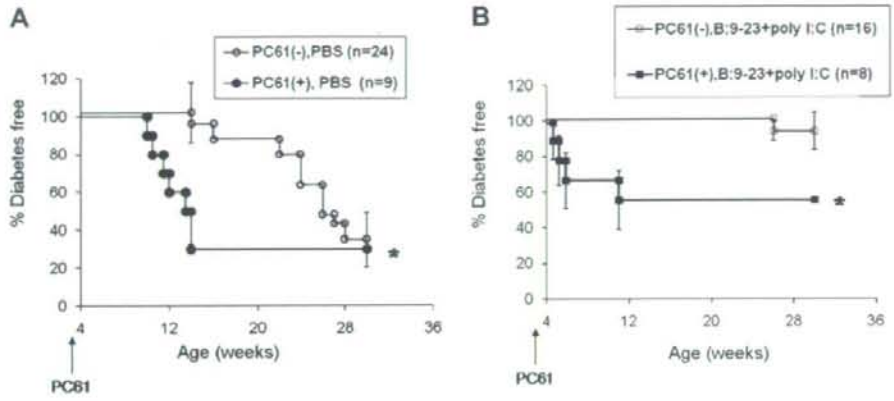

Fig. 4. (A) Life table analysis for the development of diabetes following administration of PC61 alone. Closed circles, PC61(+)PBS ($n = 9$); open circles, PC61(−)PBS ($n = 24$). $^{*}P < 0.005$. (B) Life table analysis for the development of diabetes following pre-treatment of PC61 before the combination therapy with B:9-23 peptide + poly I:C. Closed squares, PC61(+)B:9-23 + poly I:C ($n = 8$); open squares, PC61(−)B:9-23 + poly I:C ($n = 16$). $^{*}P < 0.005$.

and poly I:C, but only mild to moderate infiltration was seen in those treated with PC61 alone 2.5 weeks after PC61 injection (6 weeks of age) (Fig. 2B). Neither thyroid nor salivary glands were intact in all the mice.

These results indicate that B:9-23 peptide and poly I:C promote infiltration of both autoimmune pathogenic T cells and $Foxp3^{+}$ Tregs into the islets, and that the latter keeps the former in check, preventing development of diabetes, and following depletion of the latter with PC61 antibody diabetogenesis is remarkably accelerated.

Discussion

It has been extremely difficult to precisely define environmental determinants of type 1 diabetes of man despite early evidence that viral infections may contribute. We believe that a part of this difficulty may be dependent upon complex interplay between activation of innate and adaptive immunity, which may result in either protection or disease induction in genetically susceptible hosts. For instance, the effects of poly I:C on anti-islet autoimmunity vary in different mouse models of type 1 diabetes. Thus, our previous studies showed that poly I:C enhances anti-insulin autoimmune reaction in BALB/c mice immunized with B:9-23 peptide [8], whereas our present study (Fig. 1A) demonstrates that poly I:C does not reverse inhibitory effect of B:9-23 peptide on development of diabetes in NOD mice. Although the exact reason(s) for this difference are at present unclear, a recent study shows that the effect of poly I:C is dose-related; high dose poly I:C accelerates but low dose prevents diabetes in BioBreeding rats [17].

It was unexpected that the prevention of diabetes of NOD mice by combined poly I:C and B:9-23 peptide administration was accompanied by enhanced insulitis (Fig. 1B). Previous studies suggest that progression from insulitis to overt diabetes is regulated by Tregs in NOD mice. NOD mice only develop diabetes at 3 or 4 months of age, however, insulitis occurs long before the clinical onset of diabetes [18]. Disease transfer into irradiated recipients by spleen cells from diabetic NOD mice is prevented by $CD4^{+}$ T cells from young pre-diabetic NOD mice were co-transferred with diabetogenic T cells [19]. Recent data have indicated that this protective effect is confined to a $CD4^{+}CD25^{+}CD62L^{+}$ Treg subset [20,21].

Our immunofluorescence study indeed showed an elevated proportion of $CD4^{+}Foxp3^{+}$ T cells in the islets (but not in the PLN) from mice treated with poly I:C and B:9-23 peptide (Fig. 3). The functional significance of Tregs was verified by our depletion study, in which antibody (PC61)-mediated Treg depletion accelerated development of diabetes in untreated mice and remarkably in those treated with poly I:C and B:9-23 peptide (Fig. 4). Extremely acute onset of diabetes was observed in Treg-depleted, poly I:C and B:9-23 peptide-treated mice (Fig. 4B). Thus, PC61 antibody sensitive cells (presumably Tregs) play a role not only in suppression of spontaneous development of diabetes in untreated NOD mice, but also in mice treated with poly I:C and B:9-23 peptide. Our data indicate that combined treatment with poly I:C and insulin peptide B:9-23, recruits both pathogenic T cells and predominantly Tregs into the islets; the latter keeps the former in check, thereby suppressing progression from insulitis to diabetes. However, Treg-depletion in this situation reveals the enhanced action of the pathogenic T cells, by allowing the pathogenic T cells to infiltrate into the islet rapidly, thereby resulting in massive insulitis and acute onset diabetes.

In NOD mice, administration of insulin or insulin-derived peptides can be used to prevent diabetes [22–24] but similar approaches have failed in a clinical setting [25], possibly because of inadequate induction and accumulation of antigen-specific Tregs which can suppress the autoimmune pathogenic T cells over the long disease

course. Many therapeutic interventions with antigen-specific Tregs will be attempted to treat autoimmunity [26,27]. Our results indicate that treatment of NOD mice with insulin B:9-23 peptide, a potential primary autoantigenic epitope, and poly I:C expands the pathogenic T cells as well as Tregs and recruits them into the islets. There appear to be a fine balance between the pathogenic T cells and Tregs resulting in enhancing insulitis but suppressing progression from insulitis to overt diabetes in NOD mice. Thus, to obtain disease inhibition by an antigenic peptide vaccination, an efficient therapy which could both induce antigen-specific regulatory cell populations and purge pathogenic T cells should be considered.

Acknowledgments

We thank Dr. George S Eisenbarth (Barbara Davis Center for childhood diabetes, Denver, CO, USA) for reviewing manuscript. We also thank Y. Iwasaki, M. Motomura, and Y. Kataoka for their technical assistance and Dr. K. Yui at Nagasaki University for providing the PC61 hybridoma. This study was supported by research grants from the Japan Society for the Promotion of Science (#17590940).

References

[1] N. Abiru, G.S. Eisenbarth, Multiple genes/multiple autoantigens Role in Type 1 Diabetes, Clin. Rev. Allergy Immunol. 18 (2000) 27–40.

[2] D.R. Wegmann, M. Norbury-Glaser, D. Daniel, Insulin-specific T cells are a predominant component of islet infiltrates in pre-diabetic NOD mice, Eur. J. Immunol. 24 (1994) 1853–1857.

[3] F.S. Wong, I. Visintin, L. Wen, R.A. Flavell, C.A. Janeway, CD8 T cell clones from young nonobese diabetic (NOD) islets can transfer rapid onset of diabetes in NOD mice in the absence of CD4 cells, J. Exp. Med. 183 (1996) 67–76.

[4] H. Moriyama, N. Abiru, J. Paronen, K. Sikora, E. Liu, D. Miao, D. Devendra, J. Beilke, R. Gianani, R.G. Gill, G.S. Eisenbarth, Evidence for a primary islet autoantigen (preproinsulin 1) for insulitis and diabetes in the nonobese diabetic mouse, Proc. Natl. Acad. Sci. USA 100 (2003) 10376–10381.

[5] M. Nakayama, N. Abiru, H. Moriyama, N. Babaya, E. Liu, D. Miao, L. Yu, D.R. Wegmann, J.C. Hutton, J.F. Elliott, G.S. Eisenbarth, Prime role for an insulin epitope in the development of type 1 diabetes in NOD mice, Nature 435 (2005) 220–223.

[6] D. Daniel, D.R. Wegmann, Protection of nonobese diabetic mice from diabetes by intranasal or subcutaneous administration of insulin peptide B-(9-23), Proc. Natl. Acad. Sci. USA 93 (1996) 956–960.

[7] N. Abiru, A.K. Maniatis, L. Yu, D. Miao, H. Moriyama, D. Wegmann, G.S. Eisenbarth, Peptide and MHC-specific breaking of humoral tolerance to native insulin with the B:9-23 peptide in diabetes-prone and normal mice, Diabetes 50 (2001) 1274–1281.

[8] H. Moriyama, L. Wen, N. Abiru, E. Liu, L. Yu, D. Miao, R. Gianani, F.S. Wong, G.S. Eisenbarth, Induction and acceleration of insulitis/diabetes in mice with a viral mimic (polyinosinic–polycytidylic acid) and an insulin self-peptide, Proc. Natl. Acad. Sci. USA 99 (2002) 5539–5544.

[9] D.V. Serreze, K. Hamaguchi, E.H. Leiter, Immunostimulation circumvents diabetes in NOD/Lt mice, J. Autoimmun. 2 (1989) 759–776.

[10] W. Du, F.S. Wong, M.O. Li, J. Peng, H. Qi, R.A. Flavell, R. Sherwin, L. Wen, TGF-beta signaling is required for the function of insulin-reactive T regulatory cells, J. Clin. Invest. 116 (2006) 1360–1370.

[11] M. Belghith, J.A. Bluestone, S. Barriot, J. Megret, J.F. Bach, L. Chatenoud, TGF-beta-dependent mechanisms mediate restoration of self-tolerance induced by antibodies to CD3 in overt autoimmune diabetes, Nat. Med. 9 (2003) 1202–1208.

[12] S. Sakaguchi, Naturally arising Foxp3-expressing CD25+CD4+ regulatory T cells in immunological tolerance to self and non-self, Nat. Immunol. 6 (2005) 345–352.

[13] J.D. Fontenot, A.Y. Rudensky, A well adapted regulatory contrivance: regulatory T cell development and the forkhead family transcription factor Foxp3, Nat. Immunol. 6 (2005) 331–337.

[14] R. Mukherjee, P. Chaturvedi, H.Y. Qin, B. Singh, CD4+CD25+ regulatory T cells generated in response to insulin B:9-23 peptide prevent adoptive transfer of diabetes by diabetogenic T cells, J. Autoimmun. 21 (2003) 221–237.

[15] M. Tiittanen, J.T. Huupponen, M. Knip, O. Vaarala, Insulin treatment in patients with type 1 diabetes induces upregulation of regulatory T-cell markers in peripheral blood mononuclear cells stimulated with insulin in vitro, Diabetes 55 (2006) 3446–3454.

[16] S. Hontsu, H. Yoneyama, S. Ueha, Y. Terashima, M. Kitabatake, A. Nakano, T. Ito, H. Kimura, K. Matsushima, Visualization of naturally occurring Foxp3+ regulatory T cells in normal and tumor-bearing mice, Int. Immunopharmacol. 4 (2004) 1785–1793.

[17] D.O. Sobel, D. Goyal, B. Ahvazi, J.W. Yoon, Y.H. Chung, A. Bagg, D.M. Harlan, Low dose poly I:C prevents diabetes in the diabetes prone BB rat, J. Autoimmun. 11 (1998) 343–352.

[18] J.F. Bach, Regulatory T cells under scrutiny, Nat. Rev. Immunol. 3 (2003) 189–198.

[19] C. Boitard, R. Yasunami, M. Dardenne, J.F. Bach, T cell-mediated inhibition of the transfer of autoimmune diabetes in NOD mice, J. Exp. Med. 169 (1989) 1669–1680.

[20] V. Szanya, J. Ermann, C. Taylor, C. Holness, C.G. Fathman, The subpopulation of CD4+CD25+ splenocytes that delays adoptive transfer of diabetes expresses L-selectin and high levels of CCR7, J. Immunol. 169 (2002) 2461–2465.

[21] S. You, G. Slehoffer, S. Barriot, J.F. Bach, L. Chatenoud, Unique role of CD4+CD62L+ regulatory T cells in the control of autoimmune diabetes in T cell receptor transgenic mice, Proc. Natl. Acad. Sci. USA 101 (2004) 14580–14585.

[22] D. Daniel, R.G. Gill, N. Schloot, D. Wegmann, Epitope specificity, cytokine production profile and diabetogenic activity of insulin-specific T cell clones isolated from NOD mice, Eur. J. Immunol. 25 (1995) 1056–1062.

[23] D.G. Alleva, A. Gaur, L. Jin, D. Wegmann, P.A. Gottlieb, A. Pahuja, E.B. Johnson, T. Motheral, A. Putnam, P.D. Crowe, N. Ling, S.A. Boehme, P.J. Conlon, Immunological characterization and therapeutic activity of an altered-peptide ligand, NBI-6024, based on the immunodominant type 1 diabetes autoantigen insulin B-chain (9-23) peptide, Diabetes 51 (2002) 2126–2134.

[24] M. Kobayashi, N. Abiru, T. Arakawa, K. Fukushima, H. Zhou, E. Kawasaki, H. Yamasaki, E. Liu, D. Miao, F.S. Wong, G.S. Eisenbarth, K. Eguchi, Altered B:9-23 insulin, when administered intranasally with cholera toxin adjuvant, suppresses the expression of insulin autoantibodies and prevents diabetes, J. Immunol. 179 (2007) 2082–2088.

[25] Diabetes Prevention Trial-Type 1 Diabetes Study Group, Effects of insulin in relatives of patients with type 1 diabetes mellitus, N. Engl. J. Med. 346 (2002) 1685–1691.

[26] J.A. Bluestone, Q. Tang, Therapeutic vaccination using CD4+CD25+ antigen-specific regulatory T cells, Proc. Natl. Acad. Sci. USA 101 (2004) 14622–14626.

[27] Q. Tang, J.A. Bluestone, Regulatory T-cell physiology and application to treat autoimmunity, Immunol. Rev. 212 (2006) 217–237.

Altered B:9–23 Insulin, When Administered Intranasally with Cholera Toxin Adjuvant, Suppresses the Expression of Insulin Autoantibodies and Prevents Diabetes[1]

Masakazu Kobayashi,[2*†] Norio Abiru,[3*] Takeshi Arakawa,[‡] Keiko Fukushima,[*] Hongbo Zhou,[*] Eiji Kawasaki,[†] Hironori Yamasaki,[*] Edwin Liu,[§] Dongmei Miao,[§] F. Susan Wong,[¶] George S. Eisenbarth,[§] and Katsumi Eguchi[*]

Insulin peptide B:9–23 is a major autoantigen in type 1 diabetes that contains two distinct CD4 epitopes (B:9–16 and B:13–23). One of the two epitopes, B:13–23, overlaps with a CTL epitope (B:15–23). In this study, we report that the elimination of the CTL epitope from the B:9–23 peptide by amino acid substitution (with alanine) at positions B:16 and 19 (A16,19 altered peptide ligand) or truncation of the C-terminal amino acids from the peptide (B:9–21), neither of which stimulated the proliferation of insulin B:15–23 reactive CD8 T cells, provided significant intranasally induced suppression of diabetes when coadministered with a potent mucosal adjuvant cholera toxin (CT). Intranasal treatment with A16,19 resulted in the elimination of spontaneous insulin autoantibodies, significant inhibition of insulitis and remission from hyperglycemia, and prevented the progression to diabetes. Intranasal administration of native B:9–23/CT or B:11–23/CT resulted in a significant enhancement of insulin autoantibody expression and severity of insulitis and failed to prevent diabetes. Our present study indicates that elimination of the CTL epitope from the B:9–23 peptide was critically important for mucosally induced diabetes prevention. The A16,19 altered peptide ligand, but not other native insulin peptides, suppresses insulin autoantibodies associated with protection from and remission of diabetes. *The Journal of Immunology,* **2007, 179: 2082–2088.**

Peptide immunotherapy targeting autoreactive T cells is a potential strategy for the treatment of autoimmune diseases where an autoantigen has been identified. However, it has been suggested that mucosal administration of an autoantigenic peptide may act as a double-edged sword with the potential to induce not only protective but also pathogenic immunity, especially if a CTL epitope is present within the peptide. Martinez and coworkers suggested that the induction of CTL immunity needs to be avoided for efficient and safe diabetes prevention in mucosal peptide immunotherapy with an autoantigen, which can be accomplished by disabling the integral CTL epitopes (1). Insulin is a major target in type 1 diabetes, and the insulin B chain peptide with amino acids 9–23 (B:9–23)[4] has been suggested as a primary antigenic epitope in the pathogenesis of type 1 diabetes in NOD mice (2, 3). The B:9–23 peptide is capable of preventing diabetes in NOD mice when given s.c. (4) or as an altered peptide ligand (APL) of insulin. The peptide contains two distinct CD4 epitopes (B:9–16 and B:13–23), and B:13–23 overlaps with a CTL epitope (B:15–23) (5, 6). Insulin B:15–23 binds the K^d MHC class I molecule, with the B chain tyrosine at position 16 (binding in p2) providing the primary anchor and the glycine at position 23 (p9) providing the secondary anchor. Substitution of the tyrosine residue at position 16 with alanine or truncation from the C-terminal of B:9–23, i.e., B:9–21/22 peptide, abrogates binding of the peptide to the K^d molecule (7). An APL of B:9–23 that contains an alanine substitution at positions B:16 and B:19 (A16,19 APL) has been shown to prevent spontaneous diabetes in NOD mice when administered s.c. (8). In this study, we test the hypothesis that replacing the CTL epitope of B:9–23 with B:9–21 or A16,19 APL is superior to the native B:9–23 peptide in preventing diabetes.

We have previously demonstrated that s.c. administration of ~50 μg of B:9–23 peptide without the use of IFA induces high levels of insulin autoantibodies (IAA) in normal BALB/c mice that specifically react with intact insulin and are not absorbed by the peptide (9). However, our preliminary study showed that intranasal administration of native B:9–23 peptide (10–80 μg) failed to induce IAA in BALB/c mice. Based on our previous study that cholera toxin (CT) was able to strongly augment Th2-type humoral immunity when intranasally coadministered with a vaccine Ag

*First Department of Internal Medicine and †Department of Metabolism/Diabetes and Clinical Nutrition, Graduate School of Biomedical Sciences, Nagasaki University, Nagasaki, Japan; ‡Division of Molecular Microbiology, Center of Molecular Biosciences, University of the Ryukyus, Okinawa, Japan; §Barbara Davis Center for Childhood Diabetes, University of Colorado Health Sciences Center, Denver, CO 80262; and ¶Department of Cellular and Molecular Medicine, School of Medical Sciences, University of Bristol, Bristol, United Kingdom

Received for publication February 25, 2006. Accepted for publication May 31, 2007.

The costs of publication of this article were defrayed in part by the payment of page charges. This article must therefore be hereby marked *advertisement* in accordance with 18 U.S.C. Section 1734 solely to indicate this fact.

[1] This work was supported by research grants from Japan Society for the Promotion of Science (17590940), the Japan Diabetes Foundation (No. 14–55), and in part by a Grant-in-Aid for Scientific Research from Nagasaki University, Nagasaki, Japan.

[2] Current address: Barbara Davis Center for Childhood Diabetes, University of Colorado Health Sciences Center, Denver, CO 80262.

[3] Address correspondence and reprint requests to Dr. Norio Abiru, First Department of Internal Medicine, Graduate School of Biomedical Sciences, Nagasaki University, Sakamoto, Nagasaki, Japan. E-mail address: f1931@cc.nagasaki-u.ac.jp

[4] Abbreviations used in this paper: B:9–23, insulin B chain peptide with aa 9–23; APL, altered peptide ligand; A16,19 APL, APL with alanine substitutions at positions 16 and 19; CT, cholera toxin; IAA, insulin autoantibody; TT, tetanus toxin.

Table I. *Summary of the amino acid sequences of the insulin derived peptides studied and known epitopes for NOD islet derived T cell clones*

Peptide	Amino Acid Sequence	Reference
B:9–23	S-H-L-V-E-A-L-Y-L-V-C-G-E-R-G	
B:9–21	S-H-L-V-E-A-L-Y-L-V-C-G-E	
B:11–23	L-V-E-A-L-Y-L-V-C-G-E-R-G	
A16,19 APL	S-H-L-V-E-A-L-A-L-V-A-G-E-R-G	
Known epitopes		
For CD4 T cell clone	S-H-L-V-E-A-L-Y E-A-L-Y-L-V-C-G-E-R-G	5
For CD8 T cell clone	L-Y*-L-V-C-G-E-R-G*	6, 7

Asterisks denote residues for binding to K^d.

(10), we used CT (2 μg) as a mucosal adjuvant with the peptide and successfully induced high levels of IAA in the BALB/c mice. In this study, we evaluated the effects of disabling the CTL epitope within the B:9–23 peptide (i.e., B:9–23 derived truncated peptide and A16,19 APL) in mucosal immunization regimens on IAA induction and the development of insulitis and diabetes in NOD mice. Our results indicate that elimination of the CTL epitope from the insulin peptide B:9–23 conferred efficient suppression of insulitis and diabetes in NOD mice when the peptide was intranasally coadministered with CT. In addition, prevention of diabetes by A16,19 APL/CT was associated with the elimination of IAA expression and significant inhibition of insulitis, while treatment with the native peptide that contains the CTL epitope enhanced IAA expression without providing any protection from the disease.

Materials and Methods

Mice and antigens

Female NOD mice were purchased from Clea Japan and maintained in the Laboratory Animal Center for Biomedical Research at Nagasaki University (Nagasaki, Japan) under specific pathogen-free condition. All animal experiments described in this study were approved by the institutional animal experimentation committee and were conducted in accordance with the committee's guidelines for animal experimentation.

Mouse proinsulin II B chain-derived peptides B:9–23, B:9–21, B:11–23, A16,19 APL (Table I), and tetanus toxin (TT) peptide:830–843 (QYIKANSKFIGITE) were chemically synthesized and purified by HPLC to >95% homogeneity (purchased from Sigma-Aldrich). Insulin-related peptides and the TT peptide were dissolved in sterile saline and adjusted to a neutral pH at a concentration of 4 mg/ml. CT was purchased from List Biological Laboratories and dissolved in sterile saline at a concentration of 400 μg/ml until use.

Intranasal administration of synthetic peptides to mice

For diabetes prevention studies, mice were intranasally immunized starting at 4 wk of age (days 1–5 and 8 and then weekly until 10 wk of age) with 20 μg of peptide alone or together with 2 μg of CT. For remission studies, NOD mice at age 16–24 wk were treated with intranasal peptide administration once they were confirmed to have blood glucose levels between 200 and 249 mg/dl. The first day of intranasal treatment was counted as day 1 for this immunization regimen. Ten micrograms of the peptide was administered on days 1–5 and then twice a week for 40 days. Mice were anesthetized with ether, and 10 μl of a mixture containing the peptide and the adjuvant was slowly introduced into each nostril with a micropipette.

Measurement of antipeptide-specific Abs and IAA

Mice were bled and serum were obtained at 4, 6, 8, and 12 wk of age and stored at −20°C until the Ab assay was done. Abs against insulin peptide B:9–23 and A16,19 APL were measured by ELISA as previously described (11). Briefly, high binding Costar EIA/RIA 96-well microplates (catalog no. 3369; Corning) were coated overnight at room temperature with 1 μg of B:9–23 peptide dissolved in 100 μl of PBS per well. Wells were thoroughly washed three times with PBS and blocked with PBS containing 2% BSA and 0.01% sodium azide for a minimum of 2 h at room temperature. Wells were washed and 100 μl of 1/500 buffer-diluted serum samples were incubated for 2 h at room temperature. Wells were washed and biotin-conjugated rat anti-mouse IgG1 mAb (catalog no. 553441; BD Pharmingen) diluted 1/5000 in PBS was added to each well (100 μl/well) and incubated for 30 min. Five microliters of europium-labeled streptavidin (Wallac) was diluted in 10 ml and 100 μl was added to each well for 15 min. Wells were washed and 200 μl of enhancement solution (Wallac) was added per well and gently shaken for 10 min. Plates were analyzed by using

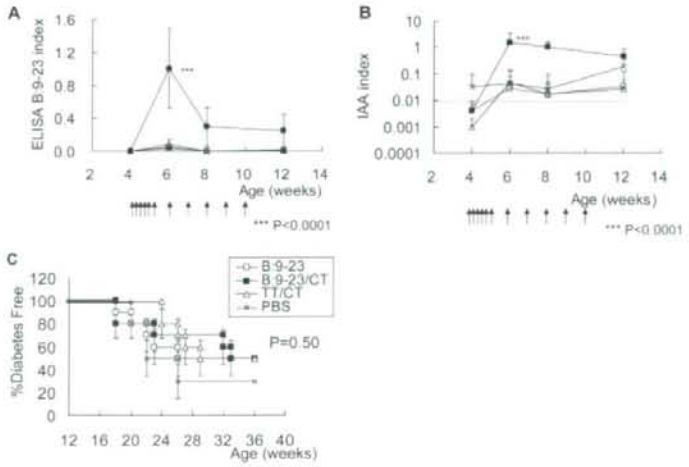

FIGURE 1. Anti-B:9–23 peptide Ab expression (*A*), IAA expression (*B*), and life table analysis for the development of diabetes (*C*) following intranasal administration of B:9–23 either alone or together with CT in NOD mice are depicted. Peptides were intranasally administered starting at 4 wk of age (days 1–5 and 8, and then weekly until 10 wk of age). □, B:9–23 alone (n = 10); ■, B:9–23/CT (n = 10); △, TT/CT (n = 10); ×, PBS, (n = 10); ***, $p < 0.0001$ vs PBS.

Table II. *Summary of peptide/CT vaccination*

Peptide	CD8 Reactivity	IAA	Insulitis	Diabetes
B:9–23/CT	↑ ↑ ↑	↑ ↑ ↑	↑ ↑ ↑	→
B:9–21/CT	→	↑	↓	↓ ↓ ↓
B:11–23/CT	↑ ↑ ↑	↑ ↑ ↑	↑ ↑ ↑	↓
A16,19 APL/CT	→	↓ ↓ ↓	↓ ↓ ↓	↓ ↓ ↓

the Victor^2 V 1420 multilabel counter (Wallac). Specific Ab levels were expressed as the index defined as follows: (sample cpm − negative control cpm)/(positive control cpm − negative control cpm).

The levels of IAA in serum were evaluated prospectively at 4, 6, 8, and 12 wk of age by using a 96-well filtration plate micro-IAA assay as previously described (12). The ^{125}I-labeled insulin Ag (Amersham Biosciences) at 20,000 cpm was incubated with 5 μl of serum with and without cold human insulin, respectively, for 3 days at 4°C in buffer A (20 mM Tris-HCl buffer (pH 7.4) containing 150 mM NaCl, 1% BSA, 0.15% Tween 20, and 0.1% sodium azide). Fifty microliters of 50% protein A with 8% protein G-Sepharose (Amersham Biosciences) was added to the serum/insulin mixture solution in a MultiScreen NOB 96-well filtration plate (Corning) that was precoated with buffer A. The plate was shaken for 45 min at 4°C followed by two cycles of four washes with cold buffer B (identical to the buffer A except for 0.1% BSA). After washing the plates, 40 μl of scintillation liquid (Microscint-20; Packard Instrument) was added to each well and radioactivity was measured by using a TopCount scintillation counter (96-well plate beta counter; Packard). The result was calculated based on the differences in counts per minute (Δcpm) between wells with and without cold insulin and expressed as an index defined as follows: (sample Δcpm − human negative control Δcpm)/(human positive control Δcpm − human negative control Δcpm). The index value of 0.01 was chosen as the cutoff limit of the normal serum level of IAA in a nondiabetic mouse strain.

Monitoring diabetes by blood glucose levels

Blood glucose levels were monitored by using Glutest-Ace (Sanwa Kagaku Kenkyusho) every other week starting at 12 wk of age for diabetes prevention studies. Mice with blood glucose levels >250 mg/dl for two consecutive measurements were considered diabetic. For remission studies, blood glucose levels were monitored twice a week for 40 days and mice having blood glucose levels >600 mg/dl or >400 mg/dl for four consecutive measurements were considered to have reached the study endpoint.

Insulin-reactive CD8 T Cells

Cloned CD8 T cells, derived from the islets of young NOD mice and designated G9C8, recognize the peptide insulin B:15–23 complex (6). A TCR transgenic mouse was generated from the TCR of the G9C8 clone on the NOD background (designated G9 transgenic mouse) and crossed to TCR$C\alpha^{-/-}$ mice to ensure that all of the TCR transgenic cells are monoclonal and express the transgenic receptor. These mice are designated G9$C\alpha^{-/-}$ NOD. The mice express CD8 T cells that respond to insulin and insulin peptide in an identical manner to that of the original clone (our unpublished observations). CD8 T cells were purified from G9$C\alpha^{-/-}$ NOD splenocytes by using positive selection beads (Miltenyi Biotec) with >95% purity for proliferation and cytotoxic assays.

Proliferation assays

Purified insulin-reactive CD8 T cells (10^5) were incubated with 10^5 irradiated NOD spleen cells together with different concentrations of peptide, in triplicate, in a 96-well round-bottom plate for 72 h. Tritiated (0.5 μCi) thymidine was added for a further 14-h incubation. The plates were harvested and thymidine uptake was measured in counts per minute using a beta plate counter.

^{51}Cr-release cytotoxicity assay

P815 cells (1×10^6) were incubated with 0.1 μCi of ^{51}Cr-labeled sodium chromate in 100 μl for 1 h, washed, and resuspended at 10^4 cells per 50 μl. The cells were incubated, in triplicate, at 25°C with different peptide concentrations in round-bottom 96-well plates for 1 h. Purified insulin-reactive CD8 T cells were added to the plate at an E:T ratio of 10:1. The cell mixture was incubated for a further 16 h at 37°C. Fifty microliters of supernatant was assayed for ^{51}Cr-release in a gamma counter. Specific lysis was determined as follows: ((cytotoxic release − minimum release)/(maximum − minimum)) × 100.

Histology

Pancreatic sections of mice immunized with insulin-related peptides were histologically analyzed at 12 wk of age by fixing tissues in 10% formalin and staining the paraffin-embedded samples with H&E. A minimum of 20 islets from each mouse were microscopically observed by two different observers for the presence of insulitis, and the levels of insulitis were scored according to the following criteria: 0, no lymphocyte infiltration; 1, islets with lymphocyte infiltration in <25% of the area; 2, 25–50% of the islet infiltrated; 3, 50–75% the islet infiltrated; 4, >75% infiltrated or small retracted islets.

Statistics analysis

Group differences were analyzed with the Tukey honestly significant difference (HSD) test and differences between Kaplan-Meier survival curves were estimated by the long rank test, with the use of Dr. SPSS II for Windows software (SPSS). Values of $p < 0.05$ were considered statistically significant. Insulitis levels were analyzed by Ridit analysis, and levels of $t > 1.96$ or < -1.96 were considered statistically significant.

Results

CT functions as an effective mucosal adjuvant for intranasally administered insulin B:9–23 peptide

Intranasal administration of 10 μg of the insulin B:9–23 peptide failed to induce anti-B:9–23-specific Abs (Fig. 1*A*). However, when the peptide was coadministered with a small amount of CT the Ab responses were significantly augmented, particularly at 6 wk of age ($p < 0.0001$ vs PBS group). The small amount of CT did not induce any obvious toxic effects. Mice given TT peptide

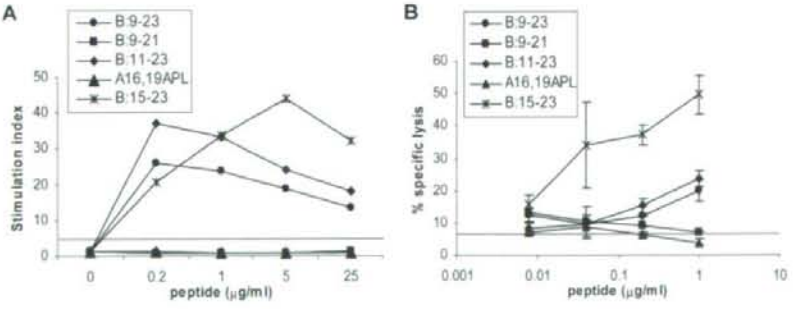

FIGURE 2. Functional responses of insulin-reactive CD8 T cells to peptides. *A*, Proliferation of insulin-reactive CD8 T cells to increasing concentrations of insulin B chain-derived peptides. The results are shown as a stimulation index (proliferation with peptide/proliferation without peptide). Background counts without peptide were 6786 + 657 cpm. *B*, ^{51}Cr-release cytotoxicity assay showing lysis of P815 targets by the insulin-reactive CD8 T cells with increasing concentrations of peptides. The horizontal line shown is the cytotoxicity in the absence of peptide. ●, B:9–23; ■, B:9–21; ♦, B:11–23,; ▲, A16,19 APL; ×, B:15–23.

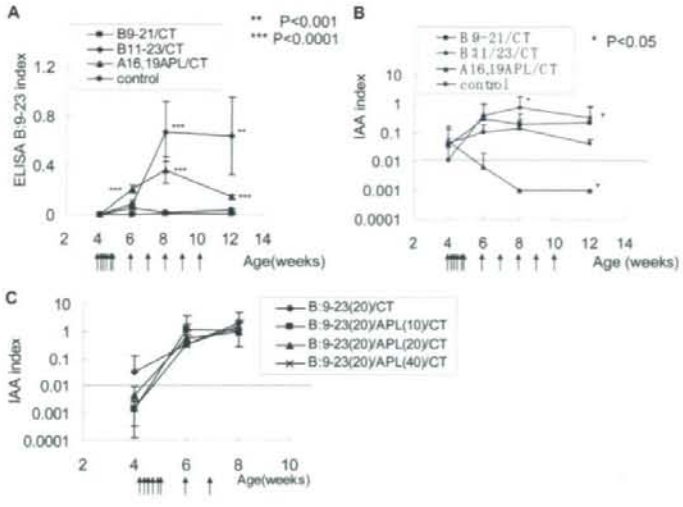

FIGURE 3. *A* and *B*, Anti-B:9–23 peptide Ab expression (*A*) and IAA expression (*B*) following intranasal administration of truncated B:9–23 and A16,19 APL together with CT in NOD mice. ■, B:9–21/CT (n = 10); ♦, B:11–23/CT (n = 9); ▲, A16,19 APL/CT (n = 8); ●, control (CT/TT and PBS) (n = 14 and 15, respectively); *, $p < 0.05$; **, $p < 0.001$; ***, $p < 0.0001$ significant vs control. *C*, IAA expression following intranasal administration of 20 μg of B:9–23 peptide/CT supplemented with different doses (0–40 μg) of A16,19 APL in NOD mice. ♦, B:9–23 peptide/CT alone (n = 10); ■, B:9–23/CT with 10 μg of APL/CT (n = 10); ▲, B:9–23/CT with 20 μg of APL/CT (n = 10); ×, B:9–23/CT with 40 μg of APL/CT (n = 10).

with CT had no effect on B:9–23 peptide-specific responses, confirming that the response was insulin peptide-specific and that CT critically influenced the level of the specific immune response.

We next examined the effects of intranasal immunization with insulin peptides on IAA. IAA can be spontaneously expressed in NOD mice as early as 4 wk of age (13). Intranasal administration of B:9–23/CT, but not B:9–23 alone or TT/CT, significantly enhanced IAA expression at 6 wk of age (Fig. 1*B* and Table II) as compared with a group given PBS ($p < 0.0001$). Based on previously reported findings that the s.c. administration of B:9–23 peptide alone induced high levels of IAA and effectively prevented diabetes in the NOD mice (14), we expected that intranasal immunization with B:9–23/CT would also prevent the development of diabetes. However, in contrast to our expectation, intranasal administration of B:9–23/CT completely failed to prevent diabetes (Fig. 1*C* and Table II). As expected, the B:9–23 peptide alone or TT/CT had no effect on the development of diabetes.

CTL epitope elimination

As described in the Introduction, the failure of disease prevention by intranasal B:9–23/CT immunization could be partly due to the induction of peptide-specific CTL immunity by the CD8 insulin B:15–23 T cell epitope. Thus, we decided to evaluate the effects of CTL epitope elimination from the B:9–23 peptide by amino acid substitutions at the B:16 and 19 positions (i.e., A16,19 APL) or by truncation of the C-terminal amino acids (i.e., B:9–21 peptide) on nasally induced Ab responses and disease prevention. To confirm whether the substitution and truncation of a CTL epitope disabled B:15–23 specific CTL immunity, proliferation and ^{51}Cr-release cytotoxicity assays of cloned insulin B:15–23 reactive CD8 T cells were performed. A comparison was made of insulin B:9–23 derived peptides with the B:15–23 peptide. As we expected, neither the A16,19 APL nor the B:9–21 peptide stimulated the proliferation of insulin-reactive CD8 T cells, while all other peptides containing the CTL epitope stimulated the CD8 T cells (Fig. 2*A*). In the proliferation, the larger peptides containing the B:15–23 epitope (B:9–23 and B:11–23) can be further processed to generate the epitope that can stimulate the CD8 T cells. In addition, as expected no cytotoxicity was stimulated by the A16,19 APL and the B:9–21 peptide. However unlike the proliferation assay, there was relatively low cytotoxicity toward targets coated with B:9–23 and B:11–23 (Fig. 2*B*). In the cytotoxicity assay, which is set up for peptides that will bind well into the K^d groove, the larger peptides are unlikely to bind appropriately to the MHC and, therefore, the stimulation of cytotoxicity using these peptides was limited.

We evaluated both Abs to the peptide B:9–23 (Fig. 3*A*) and Abs to insulin (Fig. 3*B*). Although intranasal administration of A16,19 APL/CT or B:11–23/CT induced significant levels of anti-B:9–23 Abs as compared with control, B:9–21/CT was almost completely unable to induce anti-B:9–23 Abs (Fig. 3*A* and Table II). Analyses of serum IAA revealed that significantly higher IAA was induced at 8 and 12 wk of age in mice given the B:11–23/CT group ($p < 0.05$), but not in the B:9–21/CT-immunized mice as compared with spontaneously expressed levels of IAA in the control mice. Interestingly, mice intranasally treated with A16,19 APL/CT never expressed IAA at 6, 8, and 12 wk of age except for one mouse that was IAA positive at 4 wk of age before peptide immunization (Fig. 3*B* and Table II). To test whether A16,19 APL modulated the autoimmune response to native B:9–23 peptide, we coadministered A16,19 APL and native peptide. The addition of different doses of A16,19 APL did not suppress the IAA induced by the 20-μg dose of B:9–23 peptide/CT, indicating that A16,19 APL/CT suppressed spontaneous, but not induced, autoantibody formation (Fig. 3*C*).

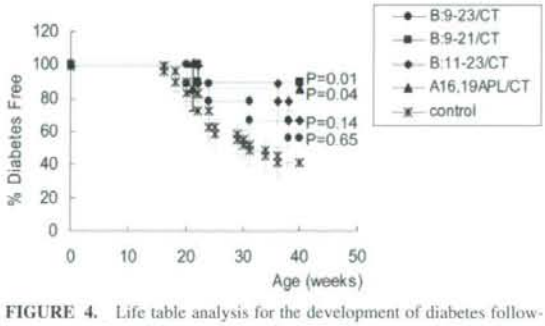

FIGURE 4. Life table analysis for the development of diabetes following intranasal administration of native B:9–23, truncated B:9–23, and A16,19 APL together with CT in NOD mice. Both intranasal-A16,19 APL/CT and intranasal-B:9–21/CT significantly suppressed the development of diabetes.

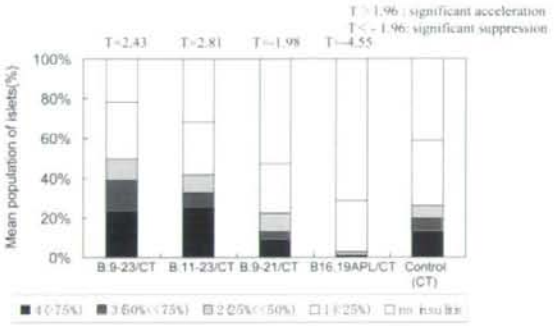

FIGURE 5. Insulitis levels at 12 wk determined by Ridit analysis. A level of $T > 1.96$ was regarded as significant increase. A level of $T < -1.96$ was regarded as significant suppression. Insulitis levels were significantly increased in the B:9–23/CT ($T = 2.43$) and B:11–23/CT ($T = 2.81$) compared with the CT alone in contrast to being suppressed slightly in the B:9–21/CT ($T = -1.98$) and strongly in the A16,19 APL/CT ($T = -4.55$).

Elimination of CTL epitope critically influenced diabetes prevention efficacy

As expected, intranasal administration of A16,19 APL/CT, or B:9–21/CT strongly suppressed the development of diabetes as compared with the control group ($p < 0.05$) (Fig. 4 and Table II). The disease prevention efficacy attained by intranasal B:11–23/CT immunization was comparable with that achieved by the A16,19 APL/CT- and B:9–21/CT-immunized groups until 34 wk of age; however, the B:11–23/CT group started to develop the disease at 40 wk of age. We also found that the blood glucose levels in most of the A16,19 APL/CT immunized mice were <100 mg/dl until 40 wk of age, whereas animals of the other groups showed blood glucose levels higher than 100 mg/dl, suggesting that the A16,19 APL was able to more effectively suppress subclinical β cell damage compared with the C-terminally truncated form of the peptide (data not shown).

Prevention of diabetes was associated with the degree of insulitis inhibition

Histological analysis of pancreatic islets of mice intranasally immunized with insulin-derived peptides revealed that B:9–23/CT and B:11–23/CT accelerated the development of insulitis as compared with the control group ($T = 2.43$ and 2.81, respectively) (Fig. 5 and Table II). In contrast, we found that administration of B:9–21/CT or A16,19 APL/CT significantly suppressed the development of insulitis ($T = -1.98$ and -4.55, respectively), and all islets of mice immunized with the A16,19 APL/CT had no insulitis or only minimal peri-insulitis (Fig. 5 and Table II).

Reversal of hyperglycemia and prevention of progression to diabetes was more often achieved by intranasal administration of the A16,19 APL than the native B:9–23 peptide

Finally, we evaluated the efficacy of insulin-derived peptides to reverse diabetes after the onset of hyperglycemia (Fig. 6). We found that 85% of the control NOD mice that became hyperglycemic (glucose levels reaching 200–249 mg/dl) eventually developed the endpoint of sustained severe hyperglycemia (>400 mg/dl) within 40 days of initial hyperglycemia. In contrast, intranasal immunization with A16,19 APL/CT resulted in remission from hyperglycemia in 65% of mice, more often than the control mice given PBS ($p < 0.05$). Native B:9–23 peptide/CT-treated mice showed a 36% remission.

Discussion

Multiple studies indicate that insulin/proinsulin is a key target in the pathogenesis of type 1 diabetes (2, 15). Several proinsulin-derived peptides, including insulin A and B chain peptides and a B-C junction peptide, have been reported to be recognized by T

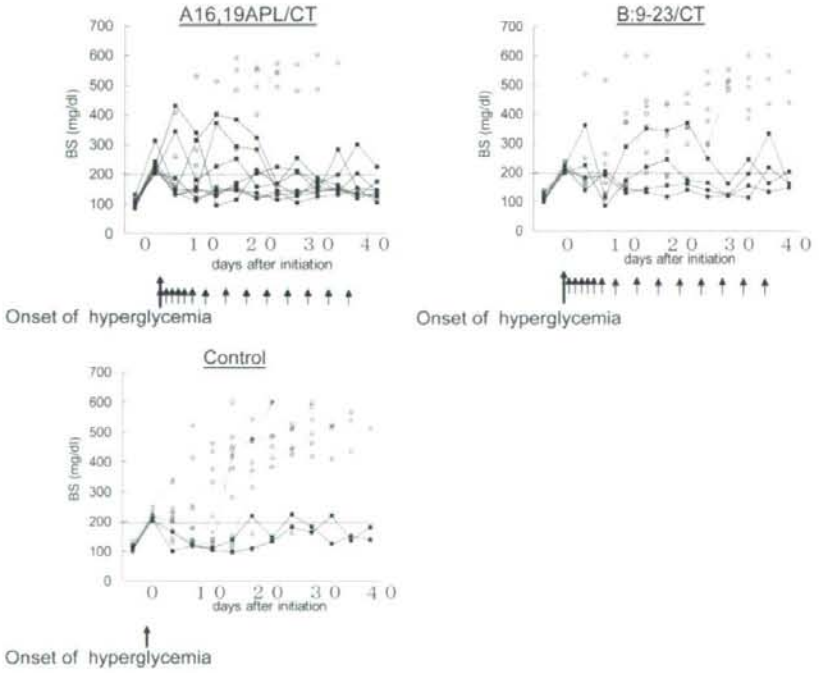

FIGURE 6. Blood glucose levels in the NOD mice intranasally treated with A16,19 APL/CT (*top left*), B:9–23/CT (*top right*), and control (*bottom left*) starting on the onset of diabetes with glucose levels between 200 mg/dl and 249 mg/dl. The peptide was intranasally immunized on days 1–5 and then twice a week until 40 days. Blood glucose levels were monitored twice a week until 40 days and we stopped the experiment at the endpoint when blood glucose levels were >600 mg/dl or 400 mg/dl four times in continuity. The mice that developed endpoint are shown as open circles (○) and others are shown as filled squares (■).

cells from humans at risk for type 1 diabetes (16, 17) and from NOD mice (15, 18). B:9–23-specific autoreactive T cell clones are found in islet infiltrates (19) and adoptively transfer diabetes into NOD SCID mice (18). The B:9–23 peptide protects NOD mice from diabetes when given subcutaneously (4, 14). With this "vaccine" NOD mice express significantly higher and long-lasting IAA compared with the levels of spontaneous IAA expression (9). Using insulin gene knockouts we have recently reported that the insulin peptide B:9–23 might be an essential target of immune destruction in the NOD mouse (3).

Mucosally induced immune regulation has been harnessed to prevent experimental autoimmune diseases, and therapeutic responses have been reported after nasal, but not oral, administration of Ags (20, 21). In this study, we found that intranasal immunization with native B:9–23 peptide in combination with CT induced significant levels of IAA without protecting against the development of diabetes in NOD mice (Fig. 1). Martinez and coworkers have reported that intranasal administration of proinsulin B24–C36 induces regulatory $CD4^+$ T cells that, however, could not inhibit the development of spontaneous diabetes in the NOD mice (1). They found that B25–C34 was a CTL epitope and that disabling it (truncation at its C terminus) inhibited diabetes (1). In this study, we have altered the B:15–23 CTL K^d epitope, previously identified (6), by truncation at the B:9–23 C terminus or amino acid substitution (alanine for tyrosine) at position B:16. Intranasal immunization with B:11–23/CT that retains the B:15–23 CD8 epitope, but not with B:9–21/CT, induced significant levels of IAA (Fig. 3*B*). This is consistent with our previous finding that one of the identified minimum epitopes, B:13–23, but not the B:9–16 epitope, induces IAA expression in normal BALB/c mice (9). Interestingly, intranasal B:11–23/CT as well as B:9–23/CT accelerated the development of insulitis but did not accelerate or inhibit diabetes development (Fig. 4). Immunization of young NOD mice with islet autoantigens such as the insulin B chain peptide prevents autoimmune diabetes (4); however, it can accelerate the development of insulitis, especially when peptides are coadministered with polyinosinic-polycytidylic acid in NOD mice (K. Fukushima, N. Abiru, and M. Kobayashi, unpublished observations). The observations made in this study and by others suggest that the B:9–23-derived peptide containing a functional CTL epitope can expand both regulatory and pathogenic T cells. In contrast to the native peptide, intranasal B:9–21/CT immunization provided significant prevention of spontaneous diabetes development with a suppressive effect on insulitis (Figs. 4 and 5) and without any effect on the spontaneous expression of IAA (Fig. 3*B*).

APLs derived from T cell-reactive self-Ags have been shown to function as protective therapeutic agents in animal models of autoimmunity. The mechanisms by which APLs may modulate immune response include antagonism (22, 23), anergy (24, 25), and immune deviation (26). Many of the analogues to date were agonistic peptides rather than antagonistic ones. B16 tyrosine is a critical amino acid for peptides that activate both NOD islet-derived $CD4^+$ and $CD8^+$ T cell clones. We previously reported that alteration of the tyrosine residue to alanine at this position abrogated the proliferative responses of anti-B:9–23 $CD4^+$ T cell clones (5). The substitution of tyrosine with alanine at the B:16 position results in the failure of the B:15–23 peptide to bind to the K^d molecule (7). Female NOD mice with a single amino acid alteration at residue 16 (from tyrosine to alanine) in the insulin B chain are dramatically protected from diabetes (3). Alleva and coworkers reported that the B:9–23-altered peptide ligand that contains alanine substitutions at residues 16 and 19, A16,19 APL (namely NBI-6024), substantially delays the onset and reduces the incidence of diabetes when given s.c. without adjuvant (8). We previously found that the induction of insulin autoantibodies is specific for the B:9–23 peptide among proinsulin-derived peptides. The Abs induced by the B:9–23 peptide react with intact insulin but are not absorbed with the peptide itself, suggesting that the B:9–23 peptide is not a B cell epitope in intact insulin and that spontaneously occurring anti-insulin B cells are activated with the help of activated T cells specific to the B:9–23 peptide (9). In our study, intranasal administration of A16,19 APL coadministered with a potent mucosal immune potentiator efficiently prevented diabetes and induced Abs reacting not only with A16,19 APL but also with the native B:9–23 peptide. Contrary to our expectation that the nasally administered A16,19 APL/CT would be associated with the enhancement of IAA expression and the acceleration of insulitis, similar to the native peptide, intranasal immunization with this peptide combined with CT completely eliminated IAA expression and strongly suppressed the development of insulitis. The inhibition of insulitis with A16,19 APL/CT should not be considered as an antagonist of the native insulin peptide binding to the K^d molecule, because A16,19 APL by itself is unable to bind MHC class I (7).

The presence of small amounts of CT was critically important for the induction of the Abs and disease prevention. Alternative adjuvants that might be safer for human use, such as a nontoxic mutant of CT or a related heat-labile toxin from enterotoxigenic *Escherichia coli* have been developed and their efficacy as mucosal adjuvants has been demonstrated (27, 28).

These studies in NOD mice demonstrate unique (native B:9–23 vs A16,19 APL) differential immunologic effects (induction vs suppression of IAA) and enhanced protection by combining the APL with specific adjuvant. Such a potent combined therapy we believe provides initial proof of concept that, with an appropriate adjuvant and a peptide, potent disease and autoantibody suppression can be achieved.

Acknowledgment

We thank Marcella Li at Barbara Davis Center for Childhood Diabetes (Denver, CO) for her technical assistance.

Disclosures

The authors have no financial conflict of interest.

References

1. Martinez, N. R., P. Augstein, A. K. Moustakas, G. K. Papadopoulos, S. Gregori, L. Adorini, D. C. Jackson, and L. C. Harrison. 2003. Disabling an integral CTL epitope allows suppression of autoimmune diabetes by intranasal proinsulin peptide. *J. Clin. Invest.* 111: 1365–1371.
2. Moriyama, H., N. Abiru, J. Paronen, K. Sikora, E. Liu, D. Miao, D. Devendra, J. Beilke, R. Gianani, R. G. Gill, and G. S. Eisenbarth. 2003. Evidence for a primary islet autoantigen (preproinsulin 1) for insulitis and diabetes in the nonobese diabetic mouse. *Proc. Natl. Acad. Sci. USA* 100: 10376–10381.
3. Nakayama, M., N. Abiru, H. Moriyama, N. Babaya, E. Liu, D. Miao, L. Yu, D. R. Wegmann, J. C. Hutton, J. F. Elliott, and G. S. Eisenbarth. 2005. Prime role for an insulin epitope in the development of type 1 diabetes in NOD mice. *Nature* 435: 220–223.
4. Daniel, D., and D. R. Wegmann. 1996. Protection of nonobese diabetic mice from diabetes by intranasal or subcutaneous administration of insulin peptide B-(9-23). *Proc. Natl. Acad. Sci. USA* 93: 956–960.
5. Abiru, N., D. Wegmann, E. Kawasaki, P. Gottlieb, E. Simone, and G. S. Eisenbarth. 2000. Dual overlapping peptides recognized by insulin peptide B:9-23 reactive T cell receptor AV13S3 T cell clones of the NOD mouse. *J. Autoimmun.* 14: 231–237.
6. Wong, F. S., J. Karttunen, C. Dumont, L. Wen, I. Visintin, I. M. Pilip, N. Shastri, E. G. Pamer, and C. A. Janeway, Jr. 1999. Identification of an MHC class I-restricted autoantigen in type 1 diabetes by screening an organ-specific cDNA library. *Nat. Med.* 5: 1026–1031.
7. Wong, F. S., A. K. Moustakas, L. Wen, G. K. Papadopoulos, and C. A. Janeway, Jr. 2002. Analysis of structure and function relationships of an autoantigenic peptide of insulin bound to H-2K(d) that stimulates CD8 T cells in insulin-dependent diabetes mellitus. *Proc. Natl. Acad. Sci. USA* 99: 5551–5556.
8. Alleva, D. G., A. Gaur, L. Jin, D. Wegmann, P. A. Gottlieb, A. Pahuja, E. B. Johnson, T. Motheral, A. Putnam, P. D. Crowe, et al. 2002. Immunological characterization and therapeutic activity of an altered-peptide ligand, NBI-6024,

based on the immunodominant type 1 diabetes autoantigen insulin B-chain (9-23) peptide. *Diabetes* 51: 2126–2134.
9. Abiru, N., A. K. Maniatis, L. Yu, D. Miao, H. Moriyama, D. Wegmann, and G. S. Eisenbarth. 2001. Peptide and MHC-specific breaking of humoral tolerance to native insulin with the B:9-23 peptide in diabetes-prone and normal mice. *Diabetes* 50: 1274–1281.
10. Arakawa, T., T. Tsuboi, A. Kishimoto, J. Sattabongkot, N. Suwanabun, T. Rungruang, Y. Matsumoto, N. Tsuji, H. Hisaeda, A. Stowers, et al. 2003. Serum antibodies induced by intranasal immunization of mice with *Plasmodium vivax* Pvs25 co-administered with cholera toxin completely block parasite transmission to mosquitoes. *Vaccine* 21: 3143–3148.
11. Liu, E., H. Moriyama, N. Abiru, D. Miao, L. Yu, R. M. Taylor, F. D. Finkelman, and G. S. Eisenbarth. 2002. Anti-peptide autoantibodies and fatal anaphylaxis in NOD mice in response to insulin self-peptides B:9-23 and B:13-23. *J. Clin. Invest.* 110: 1021–1027.
12. Yu, L., D. T. Robles, N. Abiru, P. Kaur, M. Rewers, K. Kelemen, and G. S. Eisenbarth. 2000. Early expression of anti-insulin autoantibodies of man and the NOD mouse: evidence for early determination of subsequent diabetes. *Proc. Natl. Acad. Sci. USA* 97: 1701–1706.
13. Abiru, N., L. Yu, D. Miao, A. K. Maniatis, E. Liu, H. Moriyama, and G. S. Eisenbarth. 2001. Transient insulin autoantibody expression independent of development of diabetes: comparison of NOD and NOR strains. *J. Autoimmun.* 17: 1–6.
14. Liu, E., N. Abiru, H. Moriyama, D. Miao, and G. S. Eisenbarth. 2002. Induction of insulin autoantibodies and protection from diabetes with subcutaneous insulin B:9-23 peptide without adjuvant. *Ann. NY Acad. Sci.* 958: 224–227.
15. Chen, W., I. Bergerot, J. F. Elliott, L. C. Harrison, N. Abiru, G. S. Eisenbarth, and T. L. Delovitch. 2001. Evidence that a peptide spanning the B-C junction of proinsulin is an early autoantigen epitope in the pathogenesis of type 1 diabetes. *J. Immunol.* 167: 4926–4935.
16. Kent, S. C., Y. Chen, L. Bregoli, S. M. Clemmings, N. S. Kenyon, C. Ricordi, B. J. Hering, and D. A. Hafler. 2005. Expanded T cells from pancreatic lymph nodes of type 1 diabetic subjects recognize an insulin epitope. *Nature* 435: 224–228.
17. Alleva, D. G., P. D. Crowe, L. Jin, W. W. Kwok, N. Ling, M. Gottschalk, P. J. Conlon, P. A. Gottlieb, A. L. Putnam, and A. Gaur. 2001. A disease-associated cellular immune response in type 1 diabetics to an immunodominant epitope of insulin. *J Clin. Invest.* 107: 173–180.
18. Daniel, D., R. G. Gill, N. Schloot, and D. Wegmann. 1995. Epitope specificity, cytokine production profile and diabetogenic activity of insulin-specific T cell clones isolated from NOD mice. *Eur. J. Immunol.* 25: 1056–1062.
19. Wegmann, D. R., M. Norbury-Glaser, and D. Daniel. 1994. Insulin-specific T cells are a predominant component of islet infiltrates in pre-diabetic NOD mice. *Eur. J. Immunol.* 24: 1853–1857.
20. Metzler, B., and D. C. Wraith. 1993. Inhibition of experimental autoimmune encephalomyelitis by inhalation but not oral administration of the encephalitogenic peptide: influence of MHC binding affinity. *Int. Immunol.* 5: 1159–1165.
21. von Herrath, M. G., and L. C. Harrison. 2003. Antigen-induced regulatory T cells in autoimmunity. *Nat. Rev. Immunol.* 3: 223–232.
22. De Magistris, M. T., J. Alexander, M. Coggeshall, A. Altman, F. C. Gaeta, H. M. Grey, and A. Sette. 1992. Antigen analog-major histocompatibility complexes act as antagonists of the T cell receptor. *Cell* 68: 625–634.
23. Basu, D., C. B. Williams, and P. M. Allen. 1998. In vivo antagonism of a T cell response by an endogenously expressed ligand. *Proc. Natl. Acad. Sci. USA* 95: 14332–14336.
24. Sloan-Lancaster, J., B. D. Evavold, and P. M. Allen. 1993. Induction of T-cell anergy by altered T-cell-receptor ligand on live antigen-presenting cells. *Nature* 363: 156–159.
25. Tsitoura, D. C., W. Holter, A. Cerwenka, C. M. Gelder, and J. R. Lamb. 1996. Induction of anergy in human T helper 0 cells by stimulation with altered T cell antigen receptor ligands. *J. Immunol.* 156: 2801–2808.
26. Nicholson, L. B., J. M. Greer, R. A. Sobel, M. B. Lees, and V. K. Kuchroo. 1995. An altered peptide ligand mediates immune deviation and prevents autoimmune encephalomyelitis. *Immunity* 3: 397–405.
27. Saito, M., S. Otake, M. Ohmura, M. Hirasawa, K. Takada, J. Mega, I. Takahashi, H. Kiyono, J. R. McGhee, Y. Takeda, and M. Yamamoto. 2001. Protective immunity to *Streptococcus* mutans induced by nasal vaccination with surface protein antigen and mutant cholera toxin adjuvant. *J. Infect. Dis.* 183: 823–826.
28. Yamamoto, M., J. R. McGhee, Y. Hagiwara, S. Otake, and H. Kiyono. 2001. Genetically manipulated bacterial toxin as a new generation mucosal adjuvant. *Scand. J. Immunol.* 53: 211–217.

The EMBO Journal (2007) 26, 113–122 | © 2007 European Molecular Biology Organization | All Rights Reserved 0261-4189/07
www.embojournal.org

THE EMBO JOURNAL

Cytoplasmic destruction of p53 by the endoplasmic reticulum-resident ubiquitin ligase 'Synoviolin'

Satoshi Yamasaki[1,14], Naoko Yagishita[1,14], Takeshi Sasaki[1,14], Minako Nakazawa[1,14], Yukihiro Kato[1,14], Tadayuki Yamadera[1,14], Eunkyung Bae[2,14], Sayumi Toriyama[1], Rie Ikeda[1], Lei Zhang[1], Kazuko Fujitani[1], Eunkyung Yoo[2], Kaneyuki Tsuchimochi[1], Tomohiko Ohta[3], Natsumi Araya[1], Hidetoshi Fujita[1], Satoko Aratani[1], Katsumi Eguchi[4], Setsuro Komiya[5], Ikuro Maruyama[6], Nobuyo Higashi[7], Mitsuru Sato[7], Haruki Senoo[7], Takahiro Ochi[8], Shigeyuki Yokoyama[9], Tetsuya Amano[1], Jaeseob Kim[2], Steffen Gay[10], Akiyoshi Fukamizu[11], Kusuki Nishioka[12], Keiji Tanaka[13] and Toshihiro Nakajima[1,*]

[1]Department of Genome Science, Institute of Medical Science, St Marianna University School of Medicine, Kawasaki, Japan, [2]GenExl, Inc. Biomedical Research Center, Taejon, South Korea, [3]Division of Breast and Endocrine Surgery, Institute of Medical Science, St Marianna University School of Medicine, Kawasaki, Japan, [4]The First Department of Internal Medicine, Nagasaki University School of Medicine, Nagasaki, Japan, [5]Department of Orthopedic Surgery, Kagoshima University, Faculty of Medicine, Kagoshima, Japan, [6]Department of Dermatology and Laboratory of Molecular Medicine, Kagoshima University, Faculty of Medicine, Kagoshima, Japan, [7]Department of Anatomy, Akita University School of Medicine, Akita, Japan, [8]National Hospital Organization Sagamihara National Hospital, Kanagawa, Japan, [9]Department of Biophysics and Biochemistry, Graduate School of Science, University of Tokyo, Tokyo, Japan; Protein Research Group, RIKEN Genomic Sciences Center, Yokohama, Japan, [10]Department of Rheumatology, University Hospital Zürich, Zürich, Switzerland, [11]Aspect of Functional Genomic Biology, Center of Tsukuba Advanced Research Alliance, University of Tsukuba, Tsukuba, Japan, [12]Rheumatology, Immunology and Genetics Program, Institute of Medical Science, St Marianna University School of Medicine, Kawasaki, Japan and [13]Laboratory of Frontier Science, The Tokyo Metropolitan Institute of Medical Science, Tokyo, Japan

Synoviolin, also called HRD1, is an E3 ubiquitin ligase and is implicated in endoplasmic reticulum -associated degradation. In mammals, Synoviolin plays crucial roles in various physiological and pathological processes, including embryogenesis and the pathogenesis of arthropathy. However, little is known about the molecular mechanisms of Synoviolin in these actions. To clarify these issues, we analyzed the profile of protein expression in *synoviolin*-null cells. Here, we report that Synoviolin targets tumor suppressor gene p53 for ubiquitination. Synoviolin sequestrated and metabolized p53 in the cytoplasm and negatively regulated its cellular level and biological functions, including transcription, cell cycle regulation and apoptosis. Furthermore, these p53 regulatory functions of Synoviolin were irrelevant to other E3 ubiquitin ligases for p53, such as MDM2, Pirh2 and Cop1, which form autoregulatory feedback loops. Our results provide novel insights into p53 signaling mediated by Synoviolin.

The EMBO Journal (2007) **26**, 113–122. doi:10.1038/sj.emboj.7601490; Published online 14 December 2006
Subject Categories: proteins
Keywords: apoptosis; cell growth; E3 ubiquitin ligase; endoplasmic reticulum-associated degradation; rheumatoid arthritis

Introduction

The ubiquitin–proteasome system (UPS) consists of a small polypeptide ubiquitin, a framework of enzymes that mediates the covalent attachment of ubiquitin to proteolytic substrates and the 26S proteasome that digests the modified proteins into peptides. The formation of ubiquitin conjugates requires the successive action of three classes of enzymes. This process is first activated by an E1 (activating enzyme) in an ATP-dependent manner, forming a high-energy thioester bond between ubiquitin and an E1, and the activated ubiquitin is then transferred to an E2 (conjugating enzyme), forming a similar thioester linkage between ubiquitin and E2, and then E3 ubiquitin ligase transfers ubiquitin to the target proteins. Through repeated reactions of this cycle, a polyubiquitin chain is formed on the target proteins, which is recognized by the 26S proteasome for ultimate degradation (Hershko and Ciechanover, 1998; Pickart, 2001). In the UPS pathway, the E3 ubiquitin ligases play critical roles in the selection of target proteins for degradation, because each distinct E3 ubiquitin ligase usually binds a protein substrate with a degree of selectivity for ubiquitination in a temporally and spatially regulated fashion.

Synoviolin, a representative of endoplasmic reticulum (ER)-resident E3 ubiquitin ligases, is a mammalian homolog of Hrd1p/Der3p that "substrates" misfolded carboxypeptide yscY (CPY*) (Bordallo *et al*, 1998) and 3-hydroxy-3-methylglutaryl-coenzyme A reductase (HMGR), a key enzyme of the mevalonate pathway in yeast (Shearer and Hampton, 2004, 2005). We cloned Synoviolin from rheumatoid synovial cells (RSCs) and described that Synoviolin is highly expressed in synoviocytes of patients with rheumatoid arthritis (RA) (Amano *et al*, 2003). In that report, we demonstrated that overexpression of Synoviolin in transgenic mice leads to advanced arthropathy caused by reduced apoptosis of synoviocytes. On the other hand, *synoviolin*$^{+/-}$ mice showed resistance to the development of arthritis owing to enhanced

*Corresponding author. Department of Genome Science, Institute of Medical Science, St Marianna University School of Medicine, 2-16-1 Sugao Miyamae-ku, Kawasaki, Kanagawa 216-8512, Japan. Tel.: +81 44 977 8111 (ext. 4111); Fax: +81 44 977 10712; E-mail: nakashit@marianna-u.ac.jp
[14]These authors contributed equally to this work

Received: 11 April 2006; accepted: 7 November 2006; published online: 14 December 2006

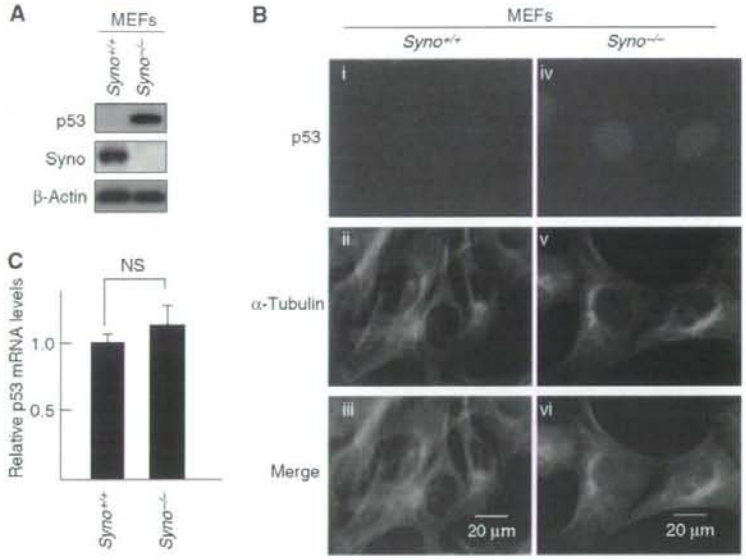

Figure 1 Accumulation of p53 in *synoviolin* null cells. (**A**) Accumulation of p53 in $Syno^{-/-}$ MEFs. (**B**) Nuclear accumulation of p53 in $Syno^{-/-}$ MEFs. p53 in $Syno^{+/+}$ MEFs (i–iii) and $Syno^{-/-}$ MEFs (iv–vi). Merged images are shown in the bottom panels (iii, vi). (**C**) Quantification of p53 mRNA. The *p53* mRNA level was assessed by real-time PCR and normalized to 18S rRNA. Data are mean±s.e.m. of four experiments. Statistical analysis using Student *t*-test indicated no significant difference between $Syno^{+/+}$ and $Syno^{-/-}$ MEFs (NS).

apoptosis of synovial cells. These results indicate that Synoviolin is a novel causative factor for arthropathy based on its anti-apoptotic effects. In another study, we reported that all mice fetuses lacking *synoviolin* ($Syno^{-/-}$) died *in utero* around E13.5 (Yagishita *et al*, 2005), although Hrd1p/Del3p, a yeast ortholog of Synoviolin, was described as non-essential for survival. $Syno^{-/-}$ were anemic owing to enhanced apoptosis of fetal liver cells (Yagishita *et al*, 2005). It is surprising that an ER-associated degradation (ERAD)-associated E3 ubiquitin ligase, Synoviolin, is involved in cell hyperplasia of dividing cells via its anti-apoptotic effect. In this regard, like RSCs, the anti-apoptotic effect of Synoviolin was observed even for *synoviolin* expressed ectopically in NIH3T3 cells, which resulted in enhanced cell overgrowth in these cells (Tsuchimochi *et al*, 2005). These results were confirmed also in the *Drosophila* fly (Supplementary Figure 1). An important question remains unanswered at this stage. What is the mechanism of Synoviolin-induced cell overgrowth? The present study was designed to identify the substrates for Synoviolin that may be involved in cell growth.

Results

Accumulation of p53 in synoviolin-null cells

To identify target(s) for Synoviolin, we assumed that the lack of Synoviolin results in accumulation of substrate proteins. First, we carried out a two-dimensional polyacrylamide gel electrophoresis (PAGE) using mouse embryonic fibroblasts (MEFs) of $Syno^{-/-}$. In these experiments, p53 was identified as one of the major targets in the profile by LC-MAS analysis (Supplementary Figure 2). Indeed, the level of p53 was markedly enhanced in $Syno^{-/-}$ MEFs (Figure 1A) and $Syno^{-/-}$ embryos, especially in the posterior part of the body such as somites, brains and maxillary or branchial arches (Supplementary Figure 3), as reported previously (Gottlieb *et al*, 1997). The accumulated p53 was predominantly localized in the nuclei of $Syno^{-/-}$ MEFs (Figure 1B), although the mRNA level of *p53* was not altered in $Syno^{-/-}$ MEFs (Figure 1C). Phosphorylation of p53 was not observed in $Syno^{-/-}$ MEFs (Supplementary Figure 4).

Increment of functional p53 in synoviolin-null cells

Next, we tested whether impairment of Synoviolin influences the functions of p53 in the cell. Knockdown of Synoviolin by small interfering RNA (siRNA) for *synoviolin* (*Syno* siRNA) in RKO cells, a human colon cancer cell line known to express wild-type (WT) p53 (Smith *et al*, 1995), resulted in almost complete disappearance of Synoviolin expression (Figure 2A). Synoviolin knockdown was associated with increased p53 protein level and nuclear accumulation of p53 (Figure 2A and B), but no change in p53 mRNA levels (Figure 2C). No changes were noted in the expression levels of other ubiquitin ligases for p53 such as MDM2, Arf-BP (data not shown) and Parc (see Figure 4B), in *synoviolin*-null RKO cells (Brooks and Gu, 2006). On the other hand, the expression levels of unfolded protein response (UPR) markers such as HERP and PERK (Wu and Kaufman, 2006) were increased, which suggests that accumulation of unfolded proteins in *synoviolin*-knockdown RKO cells caused ER stress, followed by UPR (data not shown). These results were confirmed in other cell lines (HEK293 cells and HeLa cells, data not shown). In another experiment, a marked increase was noted in the binding of p53 to its consensus sequences such as *GADD45*, *MDM2* and *p21* promoter in *synoviolin*-knockdown cells compared with *GFP*-knockdown cells (Figure 2D). Furthermore, further additions of the respective competitor abrogated the binding capacity dose-dependently, confirming the specific interactions of p53 on electrophoretic mobility

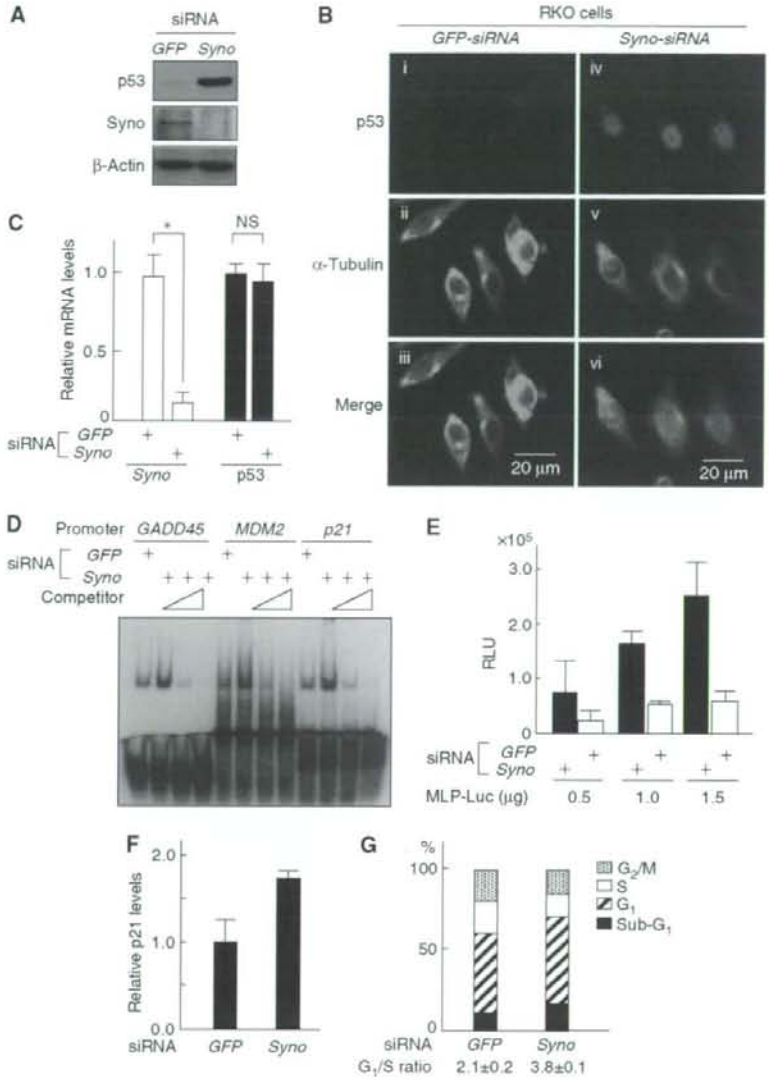

Figure 2 Functional evaluation of increased p53 in *synoviolin*-deficient RKO cells. (**A**) Increment of endogenous p53 by depletion of *synaviolin*. (**B**) Depletion of *synoviolin* causes nuclear accumulation of p53. Merged images are shown in the bottom panels (iii, vi). (**C**) *synoviolin* depletion does not affect mRNA levels of *p53*. Real-time PCR was performed as in Figure 1C. $^*P<0.01$. (**D**) DNA-binding activity of p53 for promoters of the indicated genes increases by depletion of *synoviolin*. (**E**) Transactivation activity of p53 is increased upon depletion of Synoviolin. Relative transactivation activity was determined by normalizing luciferase to an internal control, β-Gal activity from RSV-β-gal plasmid. RLU, relative light units. (**F**) siRNA depletion of *synoviolin* causes activation of p21 expression. (**G**) siRNA-induced depletion of *synoviolin* induces G_1 arrest. The cell-cycle profile was determined by propidium iodide staining and FACS. The results represent the average of triplicate experiments. Data in (C), (E) and (F) are mean ± s.e.m. of four experiments.

shift assay (EMSA) (Figure 2D). We also noted three times increment of luciferase activities on *GADD45*-MLP-Luciferase reporter plasmid in *synoviolin*-deficient RKO cells compared with *GFP*-siRNA-treated RKO cells (Figure 2E). Moreover, in *Syno* siRNA-treated RKO cells, we detected enhanced expression of p21, one of the target genes of p53 (Figure 2F), and the accumulation of cells in G_1 phase and decreased cells in S phase (Figure 2G). Taken together, the above results indicate that Synoviolin deficiency is not only associated with increased levels of p53, but also with functional activation of p53.

Synoviolin sequestrates p53 in the cytoplasm

To understand the molecular mechanism of Synoviolin-induced control of p53, we investigated the interaction between Synoviolin and p53 *in vitro*. As shown in Figure 3A, GST-SynoΔTM interacted directly with p53 (lane 8). A series of N-terminus Synoviolin-TM deletion mutants showed that the amino-acid sequence 236–270 of Synoviolin is responsible for binding with p53 (lanes 1–6) (this binding domain was termed provisionally as '53BD'). Furthermore, a synthetic 53BD peptide inhibited Synoviolin-p53 interaction in a dose-

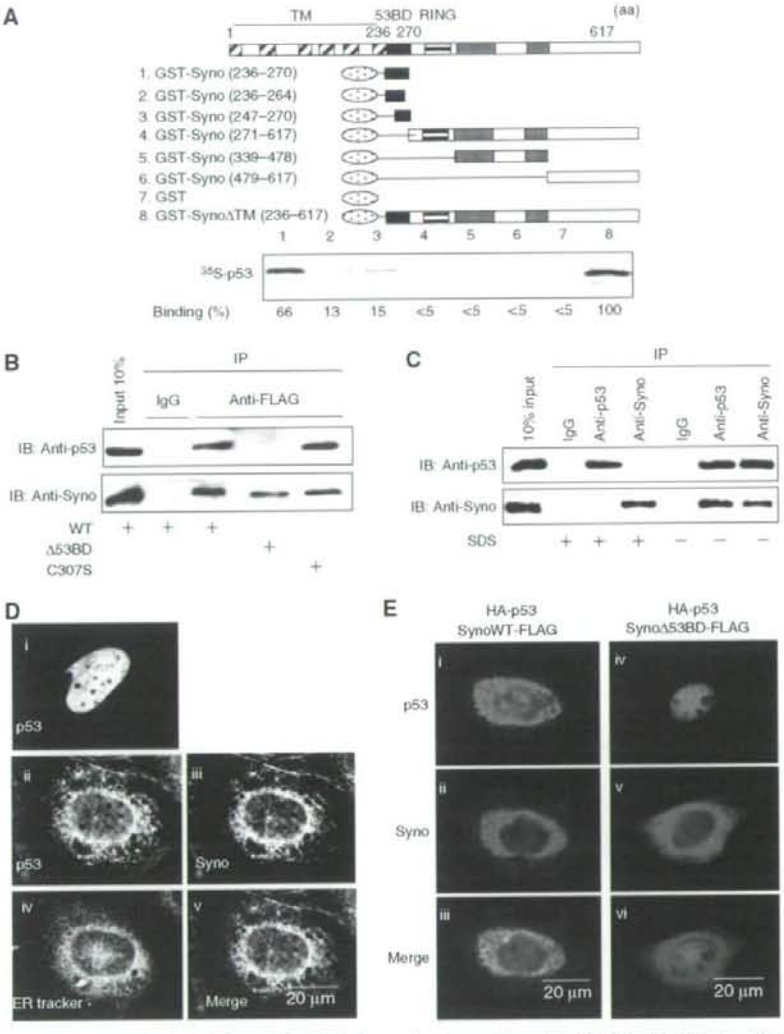

Figure 3 Synoviolin sequestrates p53 in the ER through its 53BD-dependent interaction with p53. (**A**) Identification of p53-binding domain of Synoviolin *in vitro*. Black box: p53-binding domain (53BD), gray box: proline-rich domain, oval box: GST. Relative binding ability is denoted as percentage (100% = SynoΔTM, lane 8). (**B**) 53BD-dependent *in vivo* binding of Synoviolin with p53 in HEK293 cell. (**C**) Interaction between endogenous Synoviolin and p53 in HEK293 cells. Cell lysates were immunoprecipitated in the presence or absence of SDS by using anti-p53 antibodies, anti-Synoviolin antibodies or control IgG. Inputs and immunoprecipitates were analyzed by Western blot by using anti-p53 or anti-Synoviolin antibodies. (**D**) P53 is anchored around ER in a Synoviolin-dependent manner. Saos-2 cells were transfected with HA-p53 (i) or co-transfected with HA-p53 and Synoviolin-FLAG (ii–v). Panel v shows a merged image with p53 (green), Synoviolin (red) and ER-Tracker stain (blue). (**E**) Binding of p53 with Synoviolin is required for p53 anchoring in the ER. Saos-2 cells were co-transfected with HA-p53 and Synoviolin WT-FLAG (i–iii) or SynoviolinΔ53BD-FLAG (iv–vi). Merged images are shown in the bottom panels (iii, vi).

dependent manner, whereas a peptide representing amino acids 322–332 of Synoviolin, used as a negative control, did not show any inhibitory activity (Supplementary Figure 5). We also confirmed *in vivo*, using co-immunoprecipitation assay, the interaction of transiently expressed exogenous Synoviolin WT-FLAG and p53, and the necessity of 53BD was also apparent (Figure 3B). The interaction of these two molecules was independent of ubiquitin ligase activity of Synoviolin, because Synoviolin C307S-FLAG lacking E3 activity bound to p53, as its WT (Figure 3B). Furthermore, endogenous interaction of p53 and Synoviolin was also confirmed in HEK293 cells (Figure 3C).

Considering the interplay between the ER-resident Synoviolin and the nuclear p53, we next investigated their cellular localization in Saos-2 cells, a human osteosarcoma cell line that lacks the endogenous p53 gene (Fogh *et al*, 1977), under conditions of transient expression of exogenous HA-p53 with Synoviolin WT-FLAG or SynoviolinΔ53BD-FLAG (Figure 3D and E). By overexpression of HA-p53 alone in these cells, HA-p53 was localized in the nucleus (Figure 3Di), as reported previously (Shaulsky *et al*, 1990). On the other hand, when HA-p53 was coexpressed with Synoviolin WT-FLAG, HA-p53 was predominantly colocalized with Synoviolin WT-FLAG in the perinuclear regions, but not in

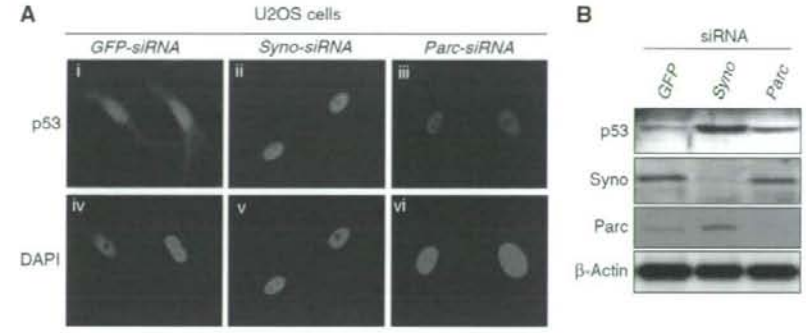

Figure 4 p53-related functional differences between Synoviolin and Parc. (**A**) Nuclear accumulation of p53 by knockdown of *synoviolin* or *Parc*. (**B**) Different levels of p53 following knockdown of *synoviolin* compared with *Parc*.

the nucleus (Figure 3Dii, iii and v). The perinuclear regions were confirmed to be the ER, by counterstaining with ER-Tracker Blue-White DPX (Figure 3Div and v). In addition, ectopically expressed SynoviolinΔ53BD-FLAG did not affect the translocation of HA-p53 into the nucleus (Figure 3E). These results clearly indicate that Synoviolin entraps p53 around ER, and that 53BD is required for this sequestration *in vivo*. In this regard, a previous study reported that another RING finger protein, Parc (Nikolaev *et al*, 2003), also acts as a cytoplasmic anchor for p53. To compare the characteristics of Synoviolin and Parc, we investigated p53 localization in U2OS cells, a human osteosarcoma cell line known to express WT p53 (Ponten and Saksela, 1967), after depletion of *synoviolin* or *Parc* (Nikolaev *et al*, 2003). Treatment with either *Syno* siRNA (Figure 4Aii and v) or *Parc* siRNA (Figure 4Aiii and vi) resulted in accumulation of p53 in the nucleus with diffused and lesser staining in the cytoplasm, different from treatment with *GFP* siRNA. Whereas the nuclear translocation of p53 was comparable in both *Syno* siRNA and *Parc* siRNA cells, a higher expression of p53 was observed in *synoviolin*-deficient U2OS cells (Figure 4Aii and iii). Western blotting analysis also revealed increased level of p53 in Synoviolin-knockdown but not in Parc-knockdown cells (Figure 4B). These findings indicate that Synoviolin regulates both localization and quantity of p53, whereas Parc does not affect the amount of p53, as reported previously (Nikolaev *et al*, 2003).

Synoviolin functions as a novel E3 ubiquitin ligase for p53 degradation

Considering that Synoviolin interacts with p53 *in vitro* and *in vivo*, we next examined whether Synoviolin ubiquitinates p53. As shown in Figure 5A, polyubiquitinated GST-p53 was detected only in the presence of ATP, PK-His-HA-Ub, E1, E2 (UbcH5c) and SynoviolinΔTM (SynoΔTM). This activity was not observed when we used Synoviolin with mutation in the RING finger domain (Figure 5B), and the deletion of 53BD also did not show any ubiquitination activity on p53 (Figure 5B), but this mutant by itself still preserved the auto-ubiquitination activity (Supplementary Figure 6). In addition, the 53BD peptide also inhibited polyubiquitination of p53 compared with a control peptide (amino acids 322–332), although the 53BD peptide did not influence the auto-ubiquitination activity of Synoviolin (Supplementary Figure 7). Moreover, ubiquitinated FLAG-p53 was observed when HA-tagged ubiquitin and Synoviolin WT were coexpressed in HEK293 cells because of its easy transfection, but Synoviolin C307S did not (Figure 5C). As a positive control, p53 was ubiquitinated by MDM2 in an *in vivo* ubiquitination assay (Figure 5C) (Haupt *et al*, 1997; Kubbutat *et al*, 1997).

In the next step, we tested the implication of ubiquitination of p53 by Synoviolin in the degradation of p53 *in vivo*. In HEK293 cells, overexpressed Synoviolin WT significantly shortened the half-life of endogenous p53, whereas Synoviolin C307S and SynoviolinΔ53BD did not increase the degradation rate of p53 (Figure 5D top, mock: 125.5 ± 18.2 min, Synoviolin WT: 44.8 ± 3.8 min, Synoviolin C307S: 177.3 ± 26.8 min and SynoviolinΔ53BD: 161.0 ± 41.4 min). These results indicate that Synoviolin is responsible for the turnover of p53 as its E3 ubiquitin ligase *in vivo*. Consistent with these data, the half-life of p53 was significantly prolonged in $Syno^{-/-}$ MEFs (Figure 5D (bottom), $Syno^{+/+}$ MEFs: 26.1 ± 1.6 min; and $Syno^{-/-}$ MEFs: 120.0 ± 30.3 min. $P<0.05$) as well as RKO cells treated with *synoviolin* siRNA (Supplementary Figure 8). In this regard, several ubiquitin ligases, such as *Cop1* (Dornan *et al*, 2004), *Pirh2* (Leng *et al*, 2003) and *MDM2* (Haupt *et al*, 1997; Kubbutat *et al*, 1997), are already reported to negatively regulate p53 (Bode and Dong, 2004). To ascertain the significance of Synoviolin relative to these ligases, we compared the effects of depletion of *synoviolin* and/or *Cop1*, *Pirh2* or *MDM2* on the expression level of p53 in RKO cells. The amount of p53 by *synoviolin* ablation was less than that by *MDM2* ablation, but equivalent to that by *Cop1* ablation. Depletion of *synoviolin* in cells treated with siRNA for *Cop1*, *Pirh2* or *MDM2* non-redundantly increased p53 levels (Figure 5E). Therefore, Synoviolin functionally targets p53 independent of other ubiquitin ligase pathways. Then, does Synoviolin regulate p53 activation process? To address this question, we applied genotoxic stress as a stimulus for p53 activation (Kastan *et al*, 1991; Vogelstein *et al*, 2000). *Syno* siRNA and *GFP* siRNA-transfected RKO cells were treated with or without genotoxic stresses such as camptothecin, actinomycin D and γ-irradiation. As expected, increased level of p53 by Synoviolin knockdown was cooperatively enhanced by treatment with genotoxic stresses in these cells (Figure 5F). Thapsigargin induced Synoviolin expression, as reported previously (Yagishita *et al*, 2005),

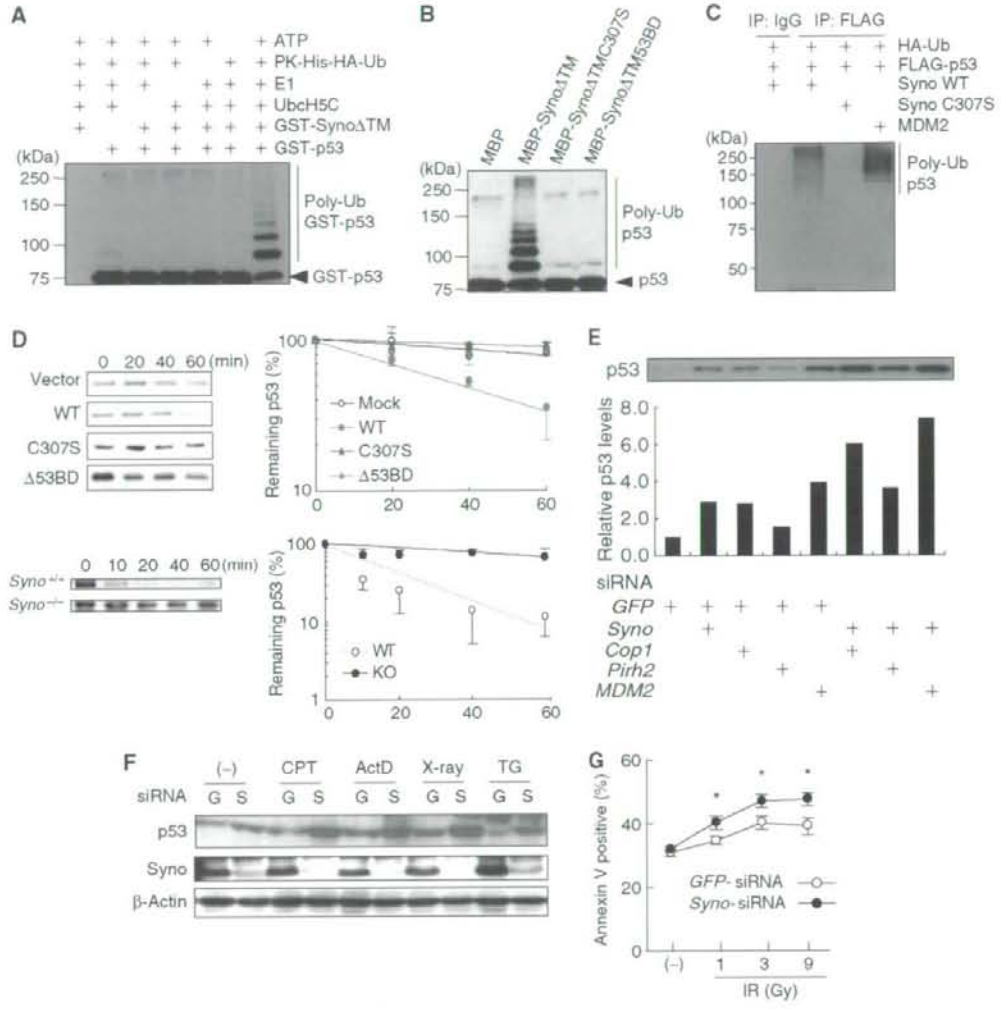

Figure 5 Synoviolin up-regulates p53 level in cells under normal and genotoxic stress conditions. (**A**) Synoviolin ubiquitinates p53 *in vitro*. (**B**) The ubiquitination of p53 is dependent on an intact RING finger domain. (**C**) WT Synoviolin, but not RING finger mutant, ubiquitinates p53 *in vivo*. (**D**) Synoviolin over-expression in HEK293 cells increases degradation of p53 (top). At 24 h after the transfection with empty vector, wild type Synoviolin (WT), mutants in RING finger domain (C307S) or p53 binding domain deletion mutant (Δ53BD), p53 expression was examined at indicated time of cycloheximide treatment. Degradation of p53 is inhibited in synoviolin knockout MEFs ($Syno^{-/-}$) compared with wild type MEFs ($Syno^{+/+}$). The p53 expression was examined after the indicated time of cycloheximide treatment. The remaining p53 expressions were normalized to β-actin expression and plotted against time (minutes). (**E**) Effects of knockdown of Synoviolin and/or other known E3 ubiquitin ligases for p53 on the level of p53 in RKO cells. Quantified p53 level is expressed as relative levels (1.0 = *GFP*-siRNA treated RKO cells). (**F**) Genotoxic stress induces p53 accumulation in the absence of Synoviolin. *GFP*- siRNA (G). *syno* siRNA (S). At 48 h after transfection, the RKO cells were treated with vehicle, camptothecine (CPT, 0.5 μM), actinomycin D (ActD, 5 nM), X-Ray (9 Gray) or thapsigargin (TG, 1 μM) for 6 h. (**G**) Synoviolin knockdown sensitizes cells to genotoxic stress. At 48 h after transfection, cells were exposed to the indicated doses of ionizing-radiation for 24 h, followed by FACS analysis to detect annexin V-positive cells. Data in (D) and (G) are mean ± s.e.m. of $n \geqslant 3$. $^*P<0.05$.

which was abolished in *Syno* siRNA-transfected RKO cells (Figure 5F). Consistent with the findings of a previous report (Qu *et al*, 2004), thapsigargin, an ER stress inducer, destabilized p53 expression compared with vehicle treatment in *GFP* siRNA-treated RKO cells. Interestingly, the thapsigargin-induced inhibition of p53 expression was reversed, at least in part, by the ablation of Synoviolin (Figure 5F). In addition, the sensitivity of *syno* siRNA-treated RKO cells to γ-irradiation was significantly increased compared with *GFP* siRNA-treated RKO cells (Figure 5G). Considered together, these results indicate that Synoviolin also participates in genotoxic stress response through the mechanism identified here.

Synoviolin regulates p53-dependent apoptotic pathway in vivo

The above experiments provided several pieces of evidence that Synoviolin is a novel class of E3 ubiquitin ligase for p53. However, the majority of the results obtained from cultured cells may not fully reflect the physiological function of p53 in

the context of the whole organism. Therefore, we used *Drosophila* to confirm the association between Synoviolin and p53. Among *Drosophila* clones, CG1937 was identified by BLASTP (protein–protein blast analysis using flybase—http://flybase.bio.indiana.edu/blast/) as the gene with 63% homology to mammalian Synoviolin, and the RING domain of CG1937 is highly conserved (82%) and *in vitro* ubiquitination assay evidently indicated that *Drosophila* Synoviolin (dSyno) ubiquitinates *Drosophila* p53 (Dmp53) (Figure 6A) (Ollmann *et al*, 2000). To investigate the role of Synoviolin in p53 regulation in the whole organism, we generated transgenic flies in which Dmp53 or dSyno was overexpressed by tissue-specific Gal4 driver (Harrison *et al*, 1995). By crossing each transgenic fly, we generated e16E-Gal4/UAS-Dmp53;UAS-dSyno/+ flies, in which both Dmp53 and dSyno could be overexpressed in the posterior halves of wings by e16E-Gal4 driver. The expression level of Dmp53 in the wing discs was significantly decreased in e16E-Gal4/UAS-Dmp53;UAS-dSyno/+ discs compared with e16E-Gal4/Dmp53;+/+ discs (Figure 6B). Moreover, acridine orange staining of apoptotic cells in these discs demonstrated that the level of apoptosis induced by overexpression of Dmp53 was diminished by dSyno overexpression (Figure 6C). These results indicate that dSyno affects Dmp53 protein levels in the fly system, similar to the results of the cell culture system.

In addition to decreased Dmp53 protein level by dSyno in the wing discs of adult flies, dSyno altered the wing phenotype. Namely, overexpression of Dmp53 by e16E-Gal4 driver caused bubbled wing phenotype at the posterior half of wings (Figure 6Di). This phenotype was completely suppressed by dSyno overexpression (Figure 6Dii and Supplementary Table 1). Overexpression of dSyno alone by e16E-Gal4 driver also produced wing phenotype (weak wrinkling of the posterior edge of the wing) (Figure 6Diii). This wrinkled phenotype

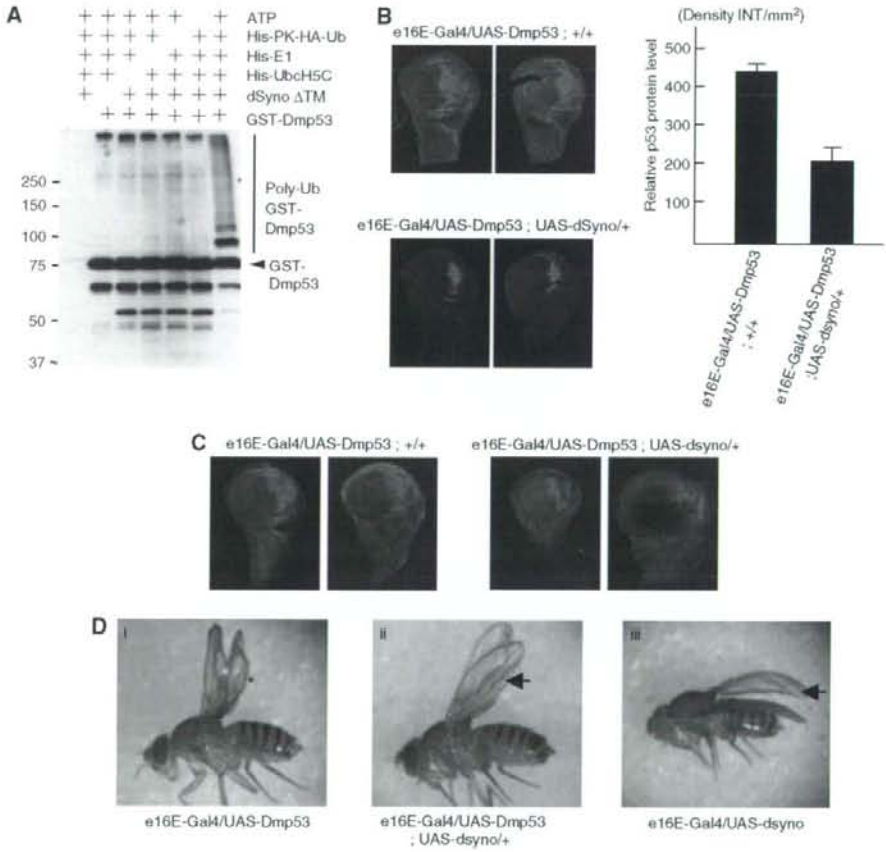

Figure 6 Synoviolin directly regulates p53-dependent apoptotic pathway in *Drosophila* fly. (**A**) Fly homolog of Synoviolin ubiquitinates fly homolog of p53 *in vitro*. GST-fusion *Drosophila melanogaster* p53 (Dmp53) was incubated with or without ATP, His-PK-HA-Ub, His-E1 (human), His-UbcH5C (human) and *Drosophila* Synoviolin (dSyno)ΔTM. Ubiquitinated proteins were probed with anti-HA antibody. (**B**) P53 protein level of wing discs was determined by immunostaining using anti-Dmp53 antibody (left). 2 representative pictures of each fly are shown. The fluorescence intensity of each 15 fly disc was quantified, and the net density level (Density INT/mm^2) was determined by subtracting the density level of the background area (anterior half of disc) from the measured level of the target area (posterior half of disc) (right). Data are mean ± s.e.m. of $n = 15$. (**C**) Apoptosis was examined by Acridine orange staining of wing disc. Overexpression of dSyno in the posterior half of the discs reduced Dmp53 overexpression-induced apoptosis. (**D**) Overexpression of dSyno suppressed the Dmp53-induced bubbled wing phenotype. The extent of wing bubble (*) in e16E-Gal4/UAS-Dmp53 flies varied with age, but the penetrance of bubbled wing phenotype was close to 100% (Supplementary Table 1). Overexpression of dSyno suppressed the Dmp53-induced bubbled wing phenotype, but dSyno-induced wrinkled phenotype at the posterior edge of wing was still observed (arrow).

induced by dSyno overexpression was not affected by Dmp53 in the double overexpressing flies (Figure 6Dii and iii, arrow). These results confirm that dSyno regulates Dmp53 protein level *in vivo* and such regulation might be accomplished through ubiquitination of dDmp53.

To determine whether this phenotypic suppression of Dmp53 by dSyno is specific to Dmp53, we investigated the interaction between dSyno and the upstream activators of p53 such as dATM, CHK2, using the same strategy. None of these activators showed interaction with dSyno (data not shown), suggesting that dSyno regulates Dmp53 protein level directly *in vivo*.

Discussion

We provide concrete evidence for the first time of the functional relationship between Synoviolin and p53. As a target for Synoviolin, p53 is evidently a non-ERAD substrate. In this regard, Doa10p, the RING finger E3 ubiquitin ligase, is known not only to be involved exclusively in removing ER proteins in the ERAD, but also to eliminate cytoplasmic targets, especially the soluble transcriptional factor Matα2, which translocates into the nucleus similar to p53 (Swanson *et al*, 2001; Laney and Hochstrasser, 2003). Thus, our finding can be viewed within the same framework of yeast though in higher eukaryotes. In the meantime, it was proposed that the ERAD in yeast is composed of two distinct surveillance mechanisms, that is, the folded state of luminal domains and the cytosolic domains are monitored by ERAD-luminal (ERAD-L) and ERAD-cytosolic (ERAD-C) pathways, respectively (Vashist and Ng, 2004; Nishikawa *et al*, 2005). Hrd1p is recognized as an ERAD-L ligase; however, this classification is not applicable to Synoviolin as a human homolog of yeast Hrd1, because Synoviolin can target both ERAD-L substrate and cytoplasmic p53 (ERAD-C substrate). Therefore, we propose the novel regulatory system of Synoviolin as a different classification of the ERAD-L/C pathway.

Maintenance of homeostasis is an important cellular function, and cells are equipped with various processes to maintain their conditions. Transcriptional alteration mediated by p53 results in a variety of cell fate changes, including growth arrest and apoptosis (Vousden and Lu, 2002; Meek, 2004). Normally, the cell maintains low levels of p53 through rapid protein degradation via the UPS by the function of ubiquitin ligases. In contrast, under genotoxic stress conditions, stabilization of p53 is promoted and the diffusely distributed p53 translocates to the nucleus owing to growth inhibition and apoptosis by its transcriptional activity. Thus, adjusting the level and nuclear localization of p53 are two essential processes for cells in order to maintain the physiological state. Although p53 mutations have been documented in more than half of all human tumors (Hollstein *et al*, 1999), it is also known that tumor cells retain WT p53. In this regard, functional inactivation of WT p53 by abnormal cytoplasmic sequestration is frequently observed in many tumor types (Moll *et al*, 1992, 1996; Schlamp *et al*, 1997). The RING finger protein Parc is considered to act as a cytoplasmic anchoring molecule of p53, but this clone does not have a p53 ubiquitination activity (Nikolaev *et al*, 2003). On the other hand, our present findings demonstrated that Synoviolin not only anchors p53 in the cytoplasm, but also ubiquitinates it, and thus differs from Parc (Figure 4). Moreover, Synoviolin diverges from other ligases for p53; each of the three ubiquitin ligases for p53 (MDM2, Pirh2 and Cop1) forms an autoregulatory negative feedback loop, resulting in lower p53 activity upon its expression, but these three ligases are target for the p53 transcriptional pathway (Dornan *et al*, 2004; Leng *et al*, 2003), whereas the expression of Synoviolin is not regulated by p53 (Figure 5F). Indeed, the *synoviolin* promoter region does not have a p53 target sequence, whereas it contains the ER stress responsive element (Tsuchimochi *et al*, 2005) and responds to the stress (Figure 5F). The reason for the multiple post-translational steps for p53 is the enormous importance of this molecule in maintaining cellular homeostasis. p53 is negatively regulated by various ubiquitin ligases, such as MDM2, MdmX, HAUSP, ARF, COP1, Pirh2 and ARF-BP1 (Brooks and Gu, 2006), and it is assumed that each molecule has its specific roles in p53 control. Among them, Synoviolin is also a unique regulator of p53 because of its independency from other ligases and transcriptional regulation by p53, ER localization and canonical function in ERAD.

In the present study, we demonstrated that Synoviolin participates in genotoxic stress-mediated p53 signaling, and its to participation in the ER stress-induced apoptosis is also well known (Bordallo *et al*, 1998; Kaneko *et al*, 2002; Kikkert *et al*, 2004; Yagishita *et al*, 2005). Therefore, Synoviolin seems to regulate two distinct apoptotic pathways and the ubiquitination of p53 by Synoviolin may be another target for crosstalk between them. Another linkage between ER stress and p53 pathway is also implicated by our finding that UPR markers are increased in cells with *synoviolin* knockdown (data not shown). Two reports described a crosstalk of p53- and ER stress- induced apoptosis pathways, that is, ER stress antagonizes p53-mediated apoptosis through the cytoplasmic localization of p53 due to phosphorylation by glycogen synthase kinase-3β (GSK-3β) (Qu *et al*, 2004), and p53 destabilization utilized the cooperative action of MDM2 and GSK-3β in ER-stressed cells (Pluquet *et al*, 2005). In this regard, it is important to note that UPR activation upon Synoviolin knockdown in RKO cells may be related to ER stress with impaired ERAD system. Since Synoviolin null cells show upregulation of p53, it is possible that the effect of p53 stabilization by Synoviolin knockdown exceeds the p53 destabilization effect of UPR induced by Synoviolin knockdown. This hypothesis may be supported by the finding that *synoviolin* siRNA treatment seemed to restore the expression of p53 at least in part, which was suppressed by ER stress (Figure 5F). The regulatory action of Synoviolin on p53 under ER stress is obviously more complex, because ER stress also induces Synoviolin expression. Further studies are necessary to determine the physiological regulatory role of Synoviolin in p53 expression under ER stress conditions.

The function of p53 in patients with RA is still controversial (Firestein *et al*, 1997; Reme *et al*, 1998; Inazuka *et al*, 2000; Muller-Ladner and Nishioka, 2000; Sun and Cheung, 2002). Mice lacking p53 do not develop spontaneous arthropathy but have severe collagen-induced arthritis (CIA) (Yamanishi *et al*, 2002; Simelyte *et al*, 2005). As we reported previously, overexpression of Synoviolin resulted in spontaneous arthropathy and its deficiency resulted in resistance to CIA in mice (Amano *et al*, 2003). Therefore, we assumed that the severity of arthritis could be determined by the Synoviolin–p53 control pathway and that the onset of spon-

taneous arthropathy may be caused by p53-independent pathway in these models. The influence of these relationships on arthritis is currently being examined in our laboratories, using *synoviolin* and p53 double null mutant mice. We hope that our research could uncover new pathogenic mechanisms of RA. Furthermore, since p53 is an important tumor suppressor gene, we believe that Synoviolin could be a useful therapeutic target for not only RA but also cancer based on its cytological and biochemical features, i.e., cytoplasmic localization and enzymatic activity (Hopkins and Groom, 2002).

In conclusion, we demonstrated that Synoviolin acts as an ERAD E3 ubiquitin ligase that controls cellular p53 and thus opens, a new concept for proliferative disorders such as RA and cancer.

Materials and methods

Plasmids

pcDNA3/Synoviolin WT or C307S-FLAG, pcDNA3/HA- and FLAG-p53, pcDNA3/MDM2 and pcDNA/HA-Ub plasmids have been described previously (Amano *et al*, 2003; Matsushita *et al*, 2005). Deletion of 53BD, MBP- and GST-fusions in Synoviolin deletion mutants was performed by PCR-based method in this study. To clone a cDNA encoding *Drosophila* homolog of human Synoviolin (dSyno), 2282 bp of CG1937 was cut out from EST GH11117 with *Eco*RI/*Xho*I, and subcloned into pUAST vector (Brand and Perrimon, 1993). The sequences of all plasmids generated by PCR were confirmed by ABI auto-sequencer.

Cells and transfections

RKO and HEK293 cells were cultured in Minimum Essential Medium (Sigma) and U2OS and Saos-2 in Dulbecco's modified Eagle's medium (Sigma). The sense sequences of siRNA oligonucleotides to *synoviolin* are (1) GGUGUUCUUUGGGCAACUG, (2) GCUGUGACAGAUGCCAUCA, (3) GGUUCUGCUGUACAUGGCC. Changes in p53 protein in RKO cells were determined by all these siRNAs. The sense sequence of siRNA oligonucleotides to *GFP* is GGCUACGUCCAGGAGCGC.

GST pull-down assay

GST-fusion proteins were expressed in *Escherichia coli* strain BL21 (Invitrogen) and purified by using glutathione-Sepharose beads (Amersham Biosciences). *In vitro*-translated ^{35}S-labeled p53 was pre-cleaned with 10 μg GST protein for 1 h at 4°C, followed by incubation with 10 μg of each GST-fusion protein in binding buffer (20 mM *N*-2-hydroxyethylpiperazine-*N'*-ethanesulfonic acid (HEPES), pH 7.9, 150 mM NaCl and 0.2% TritonX-100) for 1 h at 4°C. After washing, bound proteins were separated by SDS–PAGE and detected by BAS.

Immunoprecipitation assay

For co-immunoprecipitation assay between exogenous Synoviolin and exogenous p53, HEK293 cells were co-transfected with HA-p53 and pcDNA3-Synoviolin WT-FLAG, pcDNA3-SynoviolinΔ53BD-FLAG or pcDNA3-Synoviolin C307S-FLAG plasmids. Cell extracts were prepared with high-salt buffer (20 mM HEPES pH 7.2, 420 mM NaCl, 10% glycerol, 0.5% NP-40, 0.5 mM dithiothreitol (DTT), and 1 mM phenylmethylsulfonyl fluoride (PMSF)) and diluted at three-fold with 0.5 mM DTT and a protease inhibitor solution, followed by incubation with mouse IgG or anti-FLAG antibody. Precipitated proteins were detected by anti-HA or anti-FLAG antibodies.

To detect the interaction between endogenous Synoviolin and p53, HEK293 cells were lysed in 100 mM Tris–HCl, 80 mM NaCl, 1 mM EDTA, 5 mM EGTA, 5% glycerol, 2% (w/v) digitonin, 0.1% Brij 35, protease inhibitor cocktail and 20 μM of MG132. Immunoprecipitation was carried out in the presence or absence of SDS by using anti-p53 antibodies, anti-Synoviolin antibodies or control IgG. The immunoprecipitated samples were analyzed by western blot by using anti-p53 or anti-Synoviolin antibodies.

In vitro and in vivo ubiquitination assays

The *in vitro* ubiquitination assay was conducted as described previously (Amano *et al*, 2003). For the peptide inhibition assay, reaction solutions lacking no MBP-SynoviolinΔTM-6xHis and ATP were incubated with 53BD or control peptides (50, 100, and 200 μM) for 30 min at 4°C. Reactions were started by addition of MBP-SynoviolinΔTM-6xHis and ATP and incubating at 37°C.

For the *in vivo* ubiquitination assay, HEK293 cells were transfected with pcDNA3/HA-Ubiquitin, pcDNA3/FLAG-p53, and pcDNA3/Synoviolin WT, C307S or pcDNA3/MDM2. At 24 h post-transfection, cells were treated with MG132 (10 μM) for 1 h, then the cells were lysed in SDS containing buffer (50 mM Tris, pH 7.5, 0.5 mM EDTA, 1% SDS, and 1 mM DTT) and boiled for 5 min to denature the proteins. The denatured samples were diluted with immunoprecipitation buffer (50 mM Tris, pH 7.5, 2 mM EDTA, 150 mM NaCl, and 0.1% NP-40 and protease inhibitor cocktail) and the p53 protein was immunopurified by using anti-p53 antibody. Ubiquitinated p53 was detected by western blotting by using anti-HA antibody.

Immunostaining of fly wing discs

Fly wing discs were dissected in PBS, fixed in a buffer containing 50 mM Tris–HCl, pH 6.8, 1 mM EGTA, 1% Triton ×-100, 2 mM $MgSO_4$, 150 mM NaCl, and 2.2% formaldehyde for 15 min, and blocked using a blocking buffer (50 mM Tris–HCl, pH 6.8, 150 mM NaCl, 0.5% NP-40 and 5 mg/ml BSA). The fixed wing discs were incubated overnight at 4°C in a 1:200 dilution of anti-Dmp53 (d-200) antibody. After washing in a wash buffer (50 mM Tris–HCl, pH 6.8, 150 mM NaCl, 0.5% NP-40 and 1 mg/ml BSA), they were incubated for 3 h at 4°C in donkey anti-rabbit FITC at 1:200 dilution, washed with the wash buffer and then mounted in a mounting solution (50 mM Tris–HCl, pH 6.8, 30% glycerol, 150 mM NaCl, and 5 mg/ml phenylethylendiamine). The fluorescence intensity of each disc was quantified with Quantity One software (Bio-Rad Laboratories). Acridine orange staining was performed as reported previously (Brodsky *et al*, 2000).

Supplementary data

Supplementary data are available at *The EMBO Journal* Online (http://www.embojournal.org).

Acknowledgements

We are grateful to MR Montminy, G Verdine, R Nagata, H Shimizu, I Hishinuma, H Yokohama, H Kato, S Kitamura, K Yoshimatsu, Yuichiro ITAKURA OFFICE and ES Takagi, for advice and encouragement, and to H Takahashi, M Sato, S Otani, A Sugamiya, N Takagi, S Shinkawa, Y Nakagawa, Y Sato, M Yamanashi and members of Toshi's Laboratory for the excellent technical assistance. This study was supported in part by LocomoGene Inc., Eisai Co., Ltd, National Institute of Biomedical Innovation, the Japanese Ministry of Education, Culture, Sports, Science and Technology, the Japanese Ministry of Health, Labour and Welfare, the Kato Memorial Trust for Nanbyo Research, the Japan Medical Association, Nagao Memorial Fund, Kanae Foundation for Life & Socio-medical Science, Japan Research Foundation for Clinical Pharmacology, Kanagawa Nanbyo Foundation, Kanagawa Academy of Science and Technology Research Grants, Japan College of Rheumatology, the Nakajima Foundation, Japan Society for Promotion of Science, New Energy and Industrial Technology Development Organization, Mochida Pharmaceutical Co. Ltd, Kanto Bureau of Economy, Trade and Industry, and the Uehara Memorial Foundation. HF is supported by Japan Society for the Promotion of Science.

References

Amano T, Yamasaki S, Yagishita N, Tsuchimochi K, Shin H, Kawahara K, Aratani S, Fujita H, Zhang L, Ikeda R, Fujii R, Miura N, Komiya S, Nishioka K, Maruyama I, Fukamizu A, Nakajima T (2003) Synoviolin/Hrd1, an E3 ubiquitin ligase, as a novel pathogenic factor for arthropathy. *Genes Dev* **17:** 2436–2449

Bode AM, Dong Z (2004) Post-translational modification of p53 in tumorigenesis. *Nat Rev Cancer* **4:** 793–805

Bordallo J, Plemper RK, Finger A, Wolf DH (1998) Der3p/Hrd1p is required for endoplasmic reticulum-associated degradation of misfolded lumenal and integral membrane proteins. *Mol Biol Cell* **9:** 209–222

Brand AH, Perrimon N (1993) Targeted gene expression as a means of altering cell fates and generating dominant phenotypes. *Development* **118:** 401–415

Brodsky MH, Nordstrom W, Tsang G, Kwan E, Rubin GM, Abrams JM (2000) *Drosophila* p53 binds a damage response element at the reaper locus. *Cell* **101:** 103–113

Brooks CL, Gu W (2006) p53 ubiquitination: Mdm2 and beyond. *Mol Cell* **21:** 307–315

Dornan D, Wertz I, Shimizu H, Arnott D, Frantz GD, Dowd P, O'Rourke K, Koeppen H, Dixit VM (2004) The ubiquitin ligase COP1 is a critical negative regulator of p53. *Nature* **429:** 86–92

Firestein GS, Echeverri F, Yeo M, Zvaifler NJ, Green DR (1997) Somatic mutations in the p53 tumor suppressor gene in rheumatoid arthritis synovium. *Proc Natl Acad Sci USA* **94:** 10895–10900

Fogh J, Wright WC, Loveless JD (1977) Absence of HeLa cell contamination in 169 cell lines derived from human tumors. *J Natl Cancer Inst* **58:** 209–214

Gottlieb E, Haffner R, King A, Asher G, Gruss P, Lonai P, Oren M (1997) Transgenic mouse model for studying the transcriptional activity of the p53 protein: age- and tissue-dependent changes in radiation-induced activation during embryogenesis. *EMBO J* **16:** 1381–1390

Harrison DA, Binari R, Nahreini TS, Gilman M, Perrimon N (1995) Activation of a *Drosophila* Janus kinase (JAK) causes hematopoietic neoplasia and developmental defects. *EMBO J* **14:** 2857–2865

Haupt Y, Maya R, Kazaz A, Oren M (1997) Mdm2 promotes the rapid degradation of p53. *Nature* **387:** 296–299

Hershko A, Ciechanover A (1998) The ubiquitin system. *Annu Rev Biochem* **67:** 425–479

Hollstein M, Hergenhahn M, Yang Q, Bartsch H, Wang ZQ, Hainaut P (1999) New approaches to understanding p53 gene tumor mutation spectra. *Mutat Res* **431:** 199–209

Hopkins AL, Groom CR (2002) The druggable genome. *Nat Rev Drug Discov* **1:** 727–730

Inazuka M, Tahira T, Horiuchi T, Harashima S, Sawabe T, Kondo M, Miyahara H, Hayashi K (2000) Analysis of p53 tumour suppressor gene somatic mutations in rheumatoid arthritis synovium. *Rheumatology* **39:** 262–266

Kaneko M, Ishiguro M, Niinuma Y, Uesugi M, Nomura Y (2002) Human HRD1 protects against ER stress-induced apoptosis through ER-associated degradation. *FEBS Lett* **532:** 147–152

Kastan MB, Onyekwere O, Sidransky D, Vogelstein B, Craig RW (1991) Participation of p53 protein in the cellular response to DNA damage. *Cancer Res* **51:** 6304–6311

Kikkert M, Doolman R, Dai M, Avner R, Hassink G, vanVoorden S, Thanedar S, Roitelman J, Chau V, Wiertz E (2004) Human HRD1 is an E3 ubiquitin ligase involved in degradation of proteins from the endoplasmic reticulum. *J Biol Chem* **279:** 3525–3534

Kubbutat MH, Jones SN, Vousden KH (1997) Regulation of p53 stability by Mdm2. *Nature* **387:** 299–303

Laney JD, Hochstrasser M (2003) Ubiquitin-dependent degradation of the yeast Mat(alpha)2 repressor enables a switch in developmental state. *Genes Dev* **17:** 2259–2270

Leng RP, Lin Y, Ma W, Wu H, Lemmers B, Chung S, Parant JM, Lozano G, Hakem R, Benchimol S (2003) Pirh2, a p53-induced ubiquitin-protein ligase, promotes p53 degradation. *Cell* **112:** 779–791

Matsushita N, Kitao H, Ishiai M, Nagashima N, Hirano S, Okawa K, Ohta T, Yu DS, McHugh PJ, Hickson ID, Venkitaraman AR, Kurumizaka H, Takata M (2005) A FancD2-Monoubiquitin Fusion Reveals Hidden Functions of Fanconi Anemia Core Complex in DNA Repair. *Mol Cell* **19:** 841–847

Meek DW (2004) The p53 response to DNA damage. *DNA Repair* **3:** 1049–1056

Moll UM, Ostermeyer AG, Haladay R, Winkfield B, Frazier M, Zambetti G (1996) Cytoplasmic sequestration of wild-type p53 protein impairs the G1 checkpoint after DNA damage. *Mol Cell Biol* **16:** 1126–1137

Moll UM, Riou G, Levine AJ (1992) Two distinct mechanisms alter p53 in breast cancer: mutation and nuclear exclusion. *Proc Natl Acad Sci USA* **89:** 7262–7266

Muller-Ladner U, Nishioka K (2000) p53 in rheumatoid arthritis: friend or foe? *Arthritis Res* **2:** 175–178

Nikolaev AY, Li M, Puskas N, Qin J, Gu W (2003) Parc: a cytoplasmic anchor for p53. *Cell* **112:** 29–40

Nishikawa S, Brodsky JL, Nakatsukasa K (2005) Roles of molecular chaperones in endoplasmic reticulum (ER) quality control and ER-associated degradation (ERAD). *J Biochem* **137:** 551–555

Ollmann M, Young LM, Di Como CJ, Karim F, Belvin M, Robertson S, Whittaker K, Demsky M, Fisher WW, Buchman A, Duyk G, Friedman L, Prives C, Kopczynski C (2000) *Drosophila* p53 is a structural and functional homolog of the tumor suppressor p53. *Cell* **101:** 91–101

Pickart CM (2001) Mechanisms underlying ubiquitination. *Annu Rev Biochem* **70:** 503–533

Pluquet O, Qu L, Baltzis D, Koromilas AE (2005) Endoplasmic reticulum stress accelerates p53 degradation by the cooperative actions of Hdm2 and Glycogen synthase kinase 3β. *Mol Cell Biol* **25:** 9392–9405

Ponten J, Saksela E (1967) Two established *in vitro* cell lines from human mesenchymal tumours. *Int J Cancer* **2:** 434–447

Qu L, Huang S, Baltzis D, Rivas-Estilla AM, Pluquet O, Hatzoglou M, Koumenis C, Taya Y, Yoshimura A, Koromilas AE (2004) Endoplasmic reticulum stress induces p53 cytoplasmic localization and prevents p53-dependent apoptosis by a pathway involving glycogen synthase kinase-3beta. *Genes Dev* **18:** 261–277

Reme T, Travaglio A, Gueydon E, Adla L, Jorgensen C, Sany J (1998) Mutations of the p53 tumour suppressor gene in erosive rheumatoid synovial tissue. *Clin Exp Immunol* **111:** 353–358

Schlamp CL, Poulsen GL, Nork TM, Nickells RW (1997) Nuclear exclusion of wild-type p53 in immortalized human retinoblastoma cells. *J Natl Cancer Inst* **89:** 1530–1536

Shaulsky G, Goldfinger N, Ben-Ze'ev A, Rotter V (1990) Nuclear accumulation of p53 protein is mediated by several nuclear localization signals and plays a role in tumorigenesis. *Mol Cell Biol* **10:** 6565–6577

Shearer AG, Hampton RY (2004) Structural control of endoplasmic reticulum-associated degradation: effect of chemical chaperones on 3-hydroxy-3-methylglutaryl-CoA reductase. *J Biol Chem* **279:** 188–196

Shearer AG, Hampton RY (2005) Lipid-mediated, reversible misfolding of a sterol-sensing domain protein. *EMBO J* **24:** 149–159

Simelyte E, Rosengren S, Boyle DL, Corr M, Green DR, Firestein GS (2005) Regulation of arthritis by p53: Critical role of adaptive immunity. *Arthritis Rheum* **52:** 1876–1884

Smith ML, Chen IT, Zhan Q, O'Connor PM, Fornace Jr AJ (1995) Involvement of the p53 tumor suppressor in repair of u.v.-type DNA damage. *Oncogene* **10:** 1053–1059

Sun Y, Cheung HS (2002) p53, proto-oncogene and rheumatoid arthritis. *Semin Arthritis Rheum* **31:** 299–310

Swanson R, Locher M, Hochstrasser M (2001) A conserved ubiquitin ligase of the nuclear envelope/endoplasmic reticulum that functions in both ER-associated and Matalpha2 repressor degradation. *Genes Dev* **15:** 2660–2674

Tsuchimochi K, Yagishita N, Yamasaki S, Amano T, Kato Y, Kawahara K, Aratani S, Fujita H, Ji F, Sugiura A, Izumi T, Sugamiya A, Maruyama I, Fukamizu A, Komiya S, Nishioka K, Nakajima T (2005) Identification of a crucial site for synoviolin expression. *Mol Cell Biol* **25:** 7344–7356

Vashist S, Ng DT (2004) Misfolded proteins are sorted by a sequential checkpoint mechanism of ER quality control. *J Cell Biol* **165:** 41–52

Vogelstein B, Lane D, Levine AJ (2000) Surfing the p53 network. *Nature* **408:** 307–310

Vousden KH, Lu X (2002) Live or let die: the cell's response to p53. *Nat Rev Cancer* **2:** 594–604

Wu J, Kaufman RJ (2006) From acute ER stress to physiological roles of the Unfolded Protein Response. *Cell Death Differ* **13:** 374–384

Yagishita N, Ohneda K, Amano T, Yamasaki S, Sugiura A, Tsuchimochi K, Shin H, Kawahara K, Ohneda O, Ohta T, Tanaka S, Yamamoto M, Maruyama I, Nishioka K, Fukamizu A, Nakajima T (2005) Essential role of synoviolin in embryogenesis. *J Biol Chem* **280:** 7909–7916

Yamanishi Y, Boyle DL, Pinkoski MJ, Mahboubi A, Lin T, Han Z, Zvaifler NJ, Green DR, Firestein GS (2002) Regulation of joint destruction and inflammation by p53 in collagen-induced arthritis. *Am J Pathol* **160:** 123–130